



SUPRAGLACIAL SYSTEMS BIOLOGY OF DYNAMIC ARCTIC MICROBIAL ECOSYSTEMS

Volume 2 - Appendix

A thesis submitted for the degree of

Philosophiae Doctor

(Doctor of Philosophy)

by

Jarishma Keriuscia Gokul

(MSc, BTech (Hons), BSc)

Interdisciplinary Centre for Environmental Microbiology

Institute for Biological, Environmental and Rural Sciences

Aberystwyth University

May 2017

TABLE OF CONTENTS

TABLE OF CONTENTS	ii
LIST OF FIGURES	iii
LIST OF TABLES	iv
APPENDIX I.....	1
APPENDIX II.....	7
APPENDIX III	16
APPENDIX IV	24
APPENDIX V	42
APPENDIX VI	53

LIST OF FIGURES

APPENDIX I

Figure I. 1 Metaboanalyst statistical analysis of prominent pathways in established (control) cryoconite microcosms. Principal component analysis and hierarchical cluster analysis of the (A and B) tricarboxylic acid cycle, (C and D) amino acid metabolism and (E and F) nucleic acid biosynthesis..... 6

APPENDIX III

Figure III. 1 Multivariate analysis of Foxfonna ice cap metabolites by both (A) hierarchical cluster analysis and (B) detrended fluctuation analysis show the distinct natural clustering patterns of the metabolite separate sectors G1 and G2 from sectors G3 and G4 along a geographical demarcation point. 16

Figure III. 2 TCA cycle metabolites represented in partial least squares discriminant analysis (PLS-DA), with clear sector influence on the metabolite clustering pattern. 19

Figure III. 3 PLS-DA of polyamine metabolites show discrete metabolite clustering for each sector, with sector G1 separating into an isolated cluster..... 19

Figure III. 4 Lipid metabolite profile of ice cap cryoconite shows clustering by sector in PLS-DA, with sector G4 separating out from the other 3 sectors..... 20

Figure III. 5 There is an absence of separation in the PLS-DA for photosynthesis metabolites across the entire dome in the 95% confidence interval, with a minimal sector-bias effect..... 20

Figure III. 6 Nucleic acid metabolites show a strong sector-based east-west pattern of separation, with discrete clustering within each sector. 21

APPENDIX IV

Figure IV. 1 Standard curve of chlorophyll a..... 26

Figure IV. 2 Standard curve of mannose. 26

APPENDIX V

Figure V. 1 Pairwise Bray-Curtis distances and pairwise physical distance for sites on Greenland Ice Sheet Illulisat (DS), S6, Kangerlussuaq (KAN-P), Qaqortoq (QAS), Tasiilaq (TAS) and Thule (THU)..... 42

Figure V. 2 Meteorological data recorded by the S6 automated weather station showing conditions over the duration of the sampling season in 2014. Image credit: Dr. Tristram Irvine-Fynn. 43

LIST OF TABLES

APPENDIX I

Table I. 1 Description of cryoconite microcosm replicate tests (rep 1-3) and controls incubated over 40 days.	1
Table I. 2 Top-scoring 25 significant metabolites extracted from established cryoconite microcosms assessed by post hoc ANOVA.	3
Table I. 3 Top-scoring 50 significant metabolites extracted from newly seeded cryoconite microcosms using post hoc ANOVA.	4

APPENDIX II

Table II. 1 Environmental parameters for Foxfonna ice cap sites in Chapter 3 and Chapter 4. Aspect is in degrees (0 = N, 90 = E).	7
Table II. 2 Diversity indices for Foxfonna ice cap samples.	9
Table II. 3 Marginal tests from distLM model of environmental predictors of bacterial community structure. Aspect is in degrees (0 = N, 90 = E). SS: sums of squares; Pseudo-F: test statistic.	10
Table II. 4 Sequential tests from distLM model of environmental predictors of bacterial community structure.	10
Table II. 5 Marginal tests from distLM model of core predictors of tail population structure.	11
Table II. 6 Sequential tests from distLM model of core predictors of tail population structure.	11
Table II. 7 Marginal tests from distLM model of environmental and core OTU predictors of total population structure. Aspect is in degrees (0 = N, 90 = E).	12
Table II. 8 Sequential tests of distLM model of environmental and core OTU predictors of total community structure.	13
Table II. 9 Sequential tests of distLM model of environmental and core OTU predictors of tail community structure.	14
Table II. 10 Marginal tests from distLM model of environmental and core OTU predictors of tail population structure. Aspect is in degrees (0 = N, 90 = E).	15

APPENDIX III

Table III. 1 Tentative metabolite ID of importance established by post hoc ANOVA (P < 0.05) filtering on Metaboanalyst 3.0.	17
Table III. 2 Marginal tests of core taxa, keystone taxa and environmental parameters in redundancy analysis of total metabolites. Aspect is in degrees (0 = N, 90 = E). ...	22
Table III. 3 Sequential tests of core taxa, keystone taxa and environmental parameters in redundancy analysis of total metabolites. Aspect is in degrees (0 = N, 90 = E). ...	23

APPENDIX IV

Table IV. 1 Environmental parameters recorded on Foxfonna valley glacier. Aspect degrees (0 = N, 90 = E).	24
Table IV. 2 Sequential test of distLM model of environmental parameters on Foxfonna valley glacier.....	27
Table IV. 3 Marginal tests of distLM model of environmental parameters on Foxfonna valley glacier. Aspect is in degrees (0 = N, 90 = E).	27
Table IV. 4 Marginal tests of distLM model of environmental and high abundance bacterial taxa on the bacterial community on Foxfonna valley glacier. Aspect is in degrees (0 = N, 90 = E).	28
Table IV. 5 Sequential tests of distLM model of environmental and high abundance bacterial taxa on the bacterial community on Foxfonna valley glacier.....	28
Table IV. 6 Diversity statistics calculated for samples on Foxfonna valley glacier. ...	29
Table IV. 7 Marginal tests of distLM model predicting the effect of high abundance taxa and environmental variables on the total valley glacier bacterial community on DOY 202. Aspect is in degrees (0 = N, 90 = E).	31
Table IV. 8 Sequential tests of distLM model predicting the effect of high abundance taxa and environmental parameters on valley glacier bacterial communities on DOY 202.....	32
Table IV. 9 Marginal tests of distLM model predicting the effect of high abundance taxa and environmental parameters on valley glacier bacterial communities on DOY 210. Aspect is in degrees (0 = N, 90 = E).	32
Table IV. 10 Sequential tests of distLM model predicting the effect of high abundance taxa and environmental parameters on valley glacier bacterial communities on DOY 210.....	33
Table IV. 11 Sequential tests of distLM model predicting the effect of high abundance taxa and environmental parameters on valley glacier bacterial communities on DOY 217. Aspect is in degrees (0 = N, 90 = E).	33
Table IV. 12 Marginal tests of distLM model predicting the effect of high abundance taxa and environmental parameters on valley glacier bacterial communities on DOY 217. Aspect is in degrees (0 = N, 90 = E).	34
Table IV. 13 Marginal tests of distLM model predicting the effect of high abundance taxa and environmental parameters on valley glacier bacterial communities on DOY 221. Aspect is in degrees (0 = N, 90 = E).	35
Table IV. 14 Sequential tests of distLM model predicting the effect of high abundance taxa and environmental parameters on valley glacier bacterial communities on DOY 221. Aspect is in degrees (0 = N, 90 = E).	36
Table IV. 15 Marginal tests of distLM model predicting the effect of high abundance taxa and environmental parameters on valley glacier bacterial communities on DOY 228. Aspect is in degrees (0 = N, 90 = E).	36

Table IV. 16 Sequential tests of distLM model predicting the effect of high abundance taxa and environmental parameters on valley glacier bacterial communities on DOY 228.....	37
Table IV. 17 Marginal tests of distLM model of environmental variables, core taxa and keystone taxa on metabolites from Foxfonna glacier cryconite. Aspect is in degrees (0 = N, 90 = E).	37
Table IV. 18 Sequential tests of distLM model of environmental variables, core taxa and keystone taxa on metabolites from Foxfonna valley glacier cryconite.	38
Table IV. 19 Tentative metabolite ID of importance classified by day and site (P <0.01, FDR <0.01) established by post hoc ANOVA filtering using Metaboanalyst 3.0.....	39

APPENDIX V

Table V. 1 Diversity statistics recorded on GrIS S6.	44
Table V. 2 Marginal tests of distLM model predicting the effect of environmental conditions on 16S rRNA gene and 16S cDNA sequences on Greenland Ice Sheet surface habitats.....	47
Table V. 3 Sequential tests of distLM model predicting the effect of environmental parameters on 16S rRNA gene and 16S cDNA on Greenland Ice Sheet surfaces.	47
Table V. 4 Marginal tests of distLM model predicting the effect of environmental parameters on 16S rRNA gene and 16S cDNA cryconite on Greenland Ice Sheet. .	48
Table V. 5 Sequential tests of distLM model predicting the effect of environmental parameters on 16S rRNA gene and 16S cDNA cryconite on Greenland Ice Sheet. .	48
Table V. 6 Marginal tests of distLM model predicting the effect of environmental parameters on 16S rRNA gene and 16S cDNA snow on Greenland Ice Sheet.	49
Table V. 7 Sequential tests of distLM model predicting the effect of environmental parameters on 16S rRNA gene and 16S cDNA snow on Greenland Ice Sheet.	49
Table V. 8 Marginal tests of distLM model predicting the effect of environmental parameters on 16S rRNA gene and 16S cDNA stream on the Greenland Ice Sheet. .	50
Table V. 9 Sequential tests of distLM model predicting the effect of environmental parameters on 16S rRNA gene and 16S cDNA stream on the Greenland Ice Sheet. .	50
Table V. 10 Marginal tests of distLM model predicting the effect of environmental parameters on all active taxa in cryconite, snow and stream habitats on the Greenland Ice Sheet.	51
Table V. 11 Sequential tests of distLM model predicting the effect of environmental parameters on all active taxa in cryconite, snow and stream habitats on the Greenland Ice Sheet.	51
Table V. 12 Marginal tests of distLM model predicting the effect of environmental parameters on the rare active taxa in cryconite, snow and stream habitats on the Greenland Ice Sheet.	52
Table V. 13 Sequential tests of distLM model predicting the effect of environmental parameters on the rare active taxa in cryconite, snow and stream habitats on the Greenland Ice Sheet.	52

APPENDIX I

Supplementary data for “Chapter 3 - Morphological and metabolic characterisation of cryoconite granule development”.

Table I. 1 Description of cryoconite microcosm replicate tests (rep 1-3) and controls incubated over 40 days.

Day	Sample	Size \pm SD (L \times W, μm)	Feret Diameter (μm)	Angularity	Sphericity	Cyano- Filaments
1	rep 1	406.94 \pm 9.45 \times 335.51 \pm 5.15	423.713	Angular	High	
	rep 2	545.34 \pm 5.11 \times 364.29 \pm 1.24	556.316	Sub angular	Low	
	rep 3	928.78 \pm 3.02 \times 490.90 \pm 10.65	938.964	Very angular	Low	+
	control	570.41 \pm 5.37 \times 346.31 \pm 4.08	594.018	Very angular	Low	
5	rep 1	441.95 \pm 1.19 \times 366.75 \pm 6.72	453.762	Sub rounded	High	
	rep 2	860.47 \pm 1.52 \times 474.53 \pm 11.78	1089.639	Very angular	Low	+
	rep 3	401.88 \pm 5.31 \times 243.29 \pm 2.8	479.113	Sub angular	Low	+
	control	243.7 \pm 5.86 \times 179.91 \pm 1.31	252.46	Angular	High	
8	rep 1	373.00 \pm 6.52 \times 281.02 \pm 5.22	386.379	Very angular	Low	+
	rep 2	355.85 \pm 7.79 \times 274.83 \pm 1.35	373.175	Very angular	Low	
	rep 3	192.60 \pm 3.25 \times 166.42 \pm 5.95	209.396	Sub rounded	High	
	control	236.95 \pm 5.53 \times 197.29 \pm 3.43	274.472	Sub rounded	High	
12	rep 1	299.59 \pm 3.07 \times 195.62 \pm 1.33	313.271	Angular	High	
	rep 2	420.26 \pm 0.97 \times 147.92 \pm 2.99	429	Very angular	Low	+
	rep 3	609.20 \pm 1.79 \times 300.33 \pm 5.02	617.696	Sub angular	Low	+
	control	635.64 \pm 12.66 \times 350.92 \pm 16.00	679.157	Very angular	Low	
15	rep 1	386.64 \pm 0.76 \times 297.27 \pm 1.84	402.962	Sub angular	Low	+
	rep 2	485.69 \pm 3.34 \times 305.88 \pm 0.13	516.243	Angular	Low	+
	rep 3	241.06 \pm 1.55 \times 207.03 \pm 2.72	262.728	Angular	High	
	control	359.23 \pm 3.74 \times 221.74 \pm 1.06	366.09	Rounded	Low	
19	rep 1	430.22 \pm 11.45 \times 195.85 \pm 0.17	452.368	Angular	Low	
	rep 2	385.15 \pm 5.37 \times 324.92 \pm 0.24	409.246	Very angular	High	+
	rep 3	558.45 \pm 2.79 \times 429.80 \pm 3.24	574.749	Sub rounded	High	

Table I. 1 Description of cryoconite microcosm replicate tests (rep 1-3) and controls incubated over 40 days (continued).

Day	Sample	Size \pm SD (L \times W, μm)	Feret Diameter (μm)	Angularity	Sphericity	Cyano- Filaments
22	control	657.56 \pm 2.43 \times 338.2 \pm 6.15	681.164	Angular	Low	
	rep 1	308.00 \pm 0.98 \times 206.00 \pm 0.13	326.497	Angular	Low	+
	rep 2	502.74 \pm 0.96 \times 415.85 \pm 0.38	529.467	Very angular	Low	
	rep 3	490.35 \pm 3.34 \times 278.86 \pm 5.50	518.074	Very angular	Low	+
26	control	457.18 \pm 1.95 \times 317.2 \pm 4.70	473.106	Angular	High	
	rep 1	328.88 \pm 0.69 \times 287.14 \pm 0.58	349.298	Sub rounded	High	+
	rep 2	486.44 \pm 0.44 \times 377.65 \pm 2.33	502.487	Sub angular	Low	+
	rep 3	448.70 \pm 5.96 \times 240.28 \pm 6.17	547.076	Sub angular	Low	
29	control	546.45 \pm 7.07 \times 320.91 \pm 10.07	561.507	Sub angular	Low	
	rep 1	384.88 \pm 1.44 \times 273.66 \pm 1.18	408.197	Sub angular	Low	
	rep 2	355.95 \pm 0.24 \times 197.9 \pm 0.35	372.476	Angular	Low	
	rep 3	628.39 \pm 1.93 \times 128.27 \pm 3.29	634.106	Very angular	Low	+
33	control	522.19 \pm 5.55 \times 374.91 \pm 11.59	584.717	Sub rounded	High	
	rep 1	483.92 \pm 1.49 \times 440.86 \pm 33.07	501.167	Very angular	High	+
	rep 2	196.72 \pm 1.56 \times 140.48 \pm 0.82	217.264	Sub angular	High	+
	rep 3	348.11 \pm 5.63 \times 290.95 \pm 2.39	399.296	Very angular	High	
36	control	349.86 \pm 5.08 \times 278.93 \pm 2.29	370.665	Sub angular	High	
	rep 1	389.55 \pm 0.44 \times 254.25 \pm 0.38	421.669	Sub rounded	Low	
	rep 2	298.81 \pm 0.32 \times 202.95 \pm 0.10	324.357	Angular	High	+
	rep 3	482.83 \pm 8.63 \times 193.88 \pm 7.78	525.899	Sub angular	Low	
40	control	235.55 \pm 6.16 \times 207.00 \pm 4.46	298.839	Very angular	High	
	rep 1	405.029 \pm 2.02 \times 388.51 \pm 0.72	429.648	Angular	High	+
	rep 2	301.81 \pm 0.58 \times 167.57 \pm 1.87	326.816	Sub angular	Low	+
	rep 3	418.18 \pm 7.21 \times 140.09 \pm 4.94	470.244	Very angular	Low	
	control	192.62 \pm 2.06 \times 189.47 \pm 0.28	206.083	Rounded	High	

Table I. 2 Top-scoring 25 significant metabolites extracted from established cryoconite microcosms assessed by post hoc ANOVA.

Tentative ID	Exact mass	F value	P value	False discovery rate
Fumaric acid	115.00341	1297.3	2.59E-43	8.12E-40
Methylglyoxal	71.0134	896.85	1.94E-40	3.04E-37
Cinchonine	293.18092	528.54	2.50E-36	2.61E-33
Methanesulfonate	94.98047	514.07	4.10E-36	3.21E-33
3-hydroxy-3-methyl-2-oxobutanoate	131.0347	451.26	4.20E-35	2.63E-32
Sinapyl-alcohol	209.09505	421.17	1.44E-34	7.51E-32
Dehydroshikimate	171.06622	390.91	5.43E-34	2.43E-31
Itaconate	129.01913	369.68	1.47E-33	5.75E-31
Salicylic acid	137.02418	330.79	1.06E-32	3.69E-30
Xanthoxic acid	265.14871	300.31	5.91E-32	1.85E-29
Succinic acid	117.01904	285.09	1.49E-31	4.24E-29
2-Butenoic acid	85.0291	229.8	6.78E-30	1.77E-27
-	111.00852	228.12	7.72E-30	1.86E-27
Magnesium chloride	92.92764	214.62	2.27E-29	5.08E-27
Formic acid	128.93275	188.6	2.22E-28	4.64E-26
-	94.92475	179.67	5.22E-28	1.02E-25
Glyoxylic acid	72.99266	169.72	1.42E-27	2.62E-25
-	139.00353	166.19	2.06E-27	3.58E-25
(S)-lactaldehyde	73.02905	157.08	5.53E-27	9.12E-25
Hydroxynicotinic acid	138.01952	155.38	6.70E-27	1.05E-24
3-Cyano-L-alanine	113.02418	146.44	1.89E-26	2.78E-24
Adenosine	266.15253	146.19	1.95E-26	2.78E-24
Pyruvic acid	87.00837	145.39	2.15E-26	2.93E-24
Allophanic acid	103.03974	131.15	1.30E-25	1.70E-23
-	143.03481	124.4	3.27E-25	4.10E-23

Table I. 3 Top-scoring 50 significant metabolites extracted from newly seeded cryoconite microcosms using post hoc ANOVA.

Tentative ID	Exact mass	F value	P value	False discovery rate
succinic acid	117.019	185.27	1.51E-74	4.74E-71
S-lactaldehyde	73.02905	153.48	1.56E-69	2.44E-66
fumaric acid	115.0034	102.93	3.76E-59	3.93E-56
3-hydroxy-3-methyl-2-oxobutanoate	131.0347	99.13	3.39E-58	2.65E-55
methylglyoxal	71.0134	96.276	1.86E-57	1.17E-54
oxamic acid	88.00362	94.859	4.41E-57	2.30E-54
pyruvic acid	87.00837	82.675	1.21E-53	5.41E-51
M111.00852	111.0085	81.432	2.87E-53	1.12E-50
glyoxylic acid	72.99266	74.656	3.92E-51	1.36E-48
M139.00353	139.0035	67.037	1.59E-48	4.98E-46
N-Formimino-L-glutamate	173.082	65.983	3.81E-48	1.09E-45
M99.00839	99.00839	64.93	9.25E-48	2.42E-45
Carbamoyl phosphate	139.9987	62.175	9.96E-47	2.40E-44
3-Cyano-L-alanine	113.0242	59.623	9.74E-46	2.18E-43
Homo-cis-aconitate	187.0977	57.353	7.92E-45	1.66E-42
Aminomalonnate	118.0224	57.028	1.08E-44	2.11E-42
L-1-pyrroline-3-hydroxy-5-carboxylate	128.0351	53.154	4.60E-43	8.48E-41
salicylic acid	137.0242	50.956	4.28E-42	7.45E-40
Glyceric acid	105.019	50.693	5.62E-42	9.27E-40
M93.03425	93.03425	49.476	2.01E-41	3.15E-39
hydroxynicotinic acid	138.0195	47.94	1.04E-40	1.55E-38
R-3,3-Dimethylmalate	161.0455	47.772	1.24E-40	1.77E-38
gentisic acid	153.0192	47.588	1.52E-40	2.07E-38
hydroxypyruvic acid	102.9565	46.945	3.07E-40	4.01E-38
Allophanic acid	103.0397	46.551	4.75E-40	5.95E-38
2-oxobutanoate	100.9138	2.3321	0.011822	0.040747
valerianic acid	101.0241	37.905	1.47E-35	1.10E-33
GABA	102.0557	3.214	0.000667	0.003725
hydroxypyruvic acid	103.0033	36.531	8.94E-35	5.84E-33
urea-1-carboxylate	103.011	3.073	0.001064	0.00555
uracil	111.0197	41.152	2.50E-37	2.12E-35
3-cyanoalanine	113.0354	5.6494	2.13E-07	2.50E-06
proline	114.0558	17.573	5.00E-21	1.78E-19
aspartate-4-semialdehyde	116.0351	26.347	3.38E-28	1.82E-26
valine	116.0714	9.3238	3.10E-12	6.30E-11
homoserine	118.0508	2.8723	0.002063	0.009708
erythrose and isomers	119.0347	38.113	1.13E-35	8.62E-34
benzoic acid	121.0292	45.558	1.44E-39	1.61E-37
erythritol	121.0656	3.7936	9.65E-05	0.000665

Table I. 3 Top-scoring 50 significant metabolites extracted from newly seeded cryoconite microcosms using post hoc ANOVA (continued).

Tentative ID	Exact mass	F value	P value	False discovery rate
nicotinic acid	122.0246	35.805	2.37E-34	1.51E-32
methylcytosine	124.0402	8.675	1.99E-11	3.83E-10
thymine	125.0355	42.975	2.82E-38	2.68E-36
gamma-amino-gamma-cyanobutanoate	127.0511	3.0804	0.001039	0.005425
pipecolic acid	128.0715	2.5977	0.005052	0.020916
itaconate	129.0191	46.186	7.13E-40	8.27E-38
2-oxoisocaproic acid	129.0554	9.0091	7.60E-12	1.52E-10
glutamate-5-semialdehyde	130.0508	31.453	1.11E-31	6.68E-30
leucine	130.0871	6.6643	8.50E-09	1.21E-07
oxalacetic acid	130.9298	4.443	1.11E-05	9.42E-05
ornithine	131.0711	21.085	4.12E-24	1.79E-22

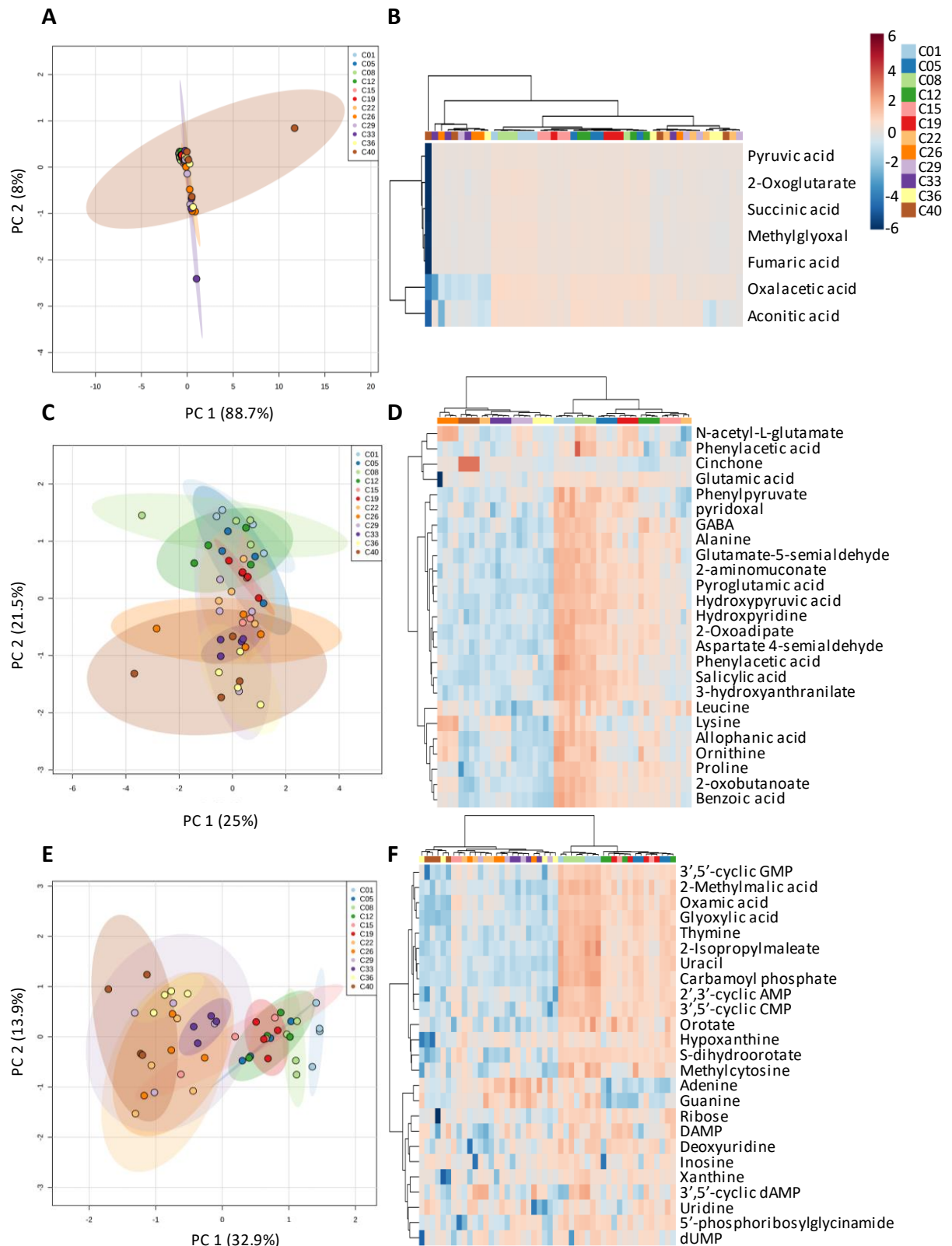


Figure I. 1 Metaboanalyst statistical analysis of prominent pathways in established (control) cryoconite microcosms. Principal component analysis and hierarchical cluster analysis of the (A and B) tricarboxylic acid cycle, (C and D) amino acid metabolism and (E and F) nucleic acid biosynthesis.

APPENDIX II

Supplementary Tables and Figures for “Chapter 4 - Bacterial biogeography of High Arctic ice cap cryoconite in Foxfonna, Svalbard”.

Table II. 1 Environmental parameters for Foxfonna ice cap sites in Chapter 3 and Chapter 4. Aspect is in degrees (0 = N, 90 = E).

Sample	Easting (UTM)	Northing (UTM)	Chl <i>a</i> ($\mu\text{g}\cdot\text{g}^{-1}$)	Z (m a.s.l.)	Slope (°)	Aspect (°)	FAA (m ²)	Flowlength (m)	Curvature	Wetness	PDD	Positive Hrs	PDH	IR (W)	IR (hrs)	ACA (%)
G1.1	526316	8672566	6.69	700.66	11.46	242.41	5075	1349.65	-8.69	0.002	77	1544	4379.384	525700	1659.413	3.41
G1.2	526293	8672774	5.16	713.43	9.84	248.24	525	108.28	0.02	0.019	77	1507	4263.233	523400	1716.781	1.86
G1.3	526380	8673063	4.04	738.02	7.64	265.13	4225	840	0.05	0.002	77	1438	4050.049	518100	1793.187	5.51
G1.4	526472	8673272	5.96	746.95	5.91	292.91	75	12.07	-4.54	0.079	77	1416	3976.312	512000	1834.854	21.71
G1.5	526630	8673519	9.09	736.29	7.4	6.65	2175	552.19	0.22	0.003	77	1443	4064.548	495000	1846	5.48
G1.6	526789	8673341	5.90	761.18	7.6	344.1	175	32.07	-1.66	0.043	77	1380	3862.573	496300	1845.288	5.53
G1.7	526670	8673046	5.97	769.58	4.8	270.38	2650	525	-4.88	0.002	77	1354	3797.409	520800	1821.7	5.01
G2.1	526733	8672710	11.86	765.8	5.97	235	875	240.42	-3.31	0.007	77	1366	3826.553	529400	1756.218	10.63
G2.2	526835	8672646	10.71	770.32	5.18	225.56	2425	678.82	0.02	0.002	77	1351	3791.765	530900	1771.812	5.00
G2.3	526895	8672534	8.18	766.07	5.09	212.24	625	169.71	-1.54	0.008	77	1366	3824.462	532600	1761.852	9.53
G2.4	526972	8672534	7.70	769.9	3.9	200.16	100	15	1.03	0.039	77	1352	3794.966	531600	1769.667	6.54
G2.5	527013	8672440	5.83	763.33	5.37	190.19	850	165	0.07	0.006	77	1372	3845.741	535500	1751.206	9.02
G2.6	526890	8672376	9.62	753.78	6.12	213.92	325	80.71	0.09	0.019	77	1392	3921.195	533500	1747.307	10.75
G2.7	526777	8672378	10.56	745.87	7.01	225.11	900	245.42	0.01	0.008	77	1416	3985.142	532000	1734.619	9.69
G2.8	526668	8672418	5.41	738.35	8.88	227.49	1400	388.91	0.04	0.006	77	1437	4047.29	533200	1696.279	7.15
G2.9	526877	8672788	5.57	781.12	4.12	240.82	1400	378.55	-3.37	0.003	77	1311	3711.535	527400	1796.238	2.24
G3.1	527537	8672831	7.82	775.99	8.45	142.28	725	197.99	0.3	0.012	77	1329	3749.182	539000	1691.426	4.95
G3.2	527486	8672736	9.19	768.83	9.67	137.37	775	212.13	-3	0.012	77	1359	3803.153	538700	1659.639	4.42
G3.3	527045	8672191	13.11	742.79	4.51	175.76	2475	490	0.12	0.002	77	1424	4010.474	532200	1767.155	5.36
G3.5	527145	8672345	15.39	753.08	6.43	152.94	150	35.36	0.12	0.043	77	1394	3926.782	535700	1736.175	3.54

Table II. 1 Environmental parameters for Foxfonna ice cap sites. Aspect is in degrees (0 = N, 90 = E) (continued).

Sample	Easting (UTM)	Northing (UTM)	Chl α ($\mu\text{g}\cdot\text{g}^{-1}$)	Z (m a.s.l.)	Slope (°)	Aspect (°)	FAA (m^2)	Flowlength (m)	Curvature	Wetness	PDD	Positive Hrs	PDH	IR (W)	IR (hrs)	ACA (%)
G3.6	527187	8672514	6.20	767.4	6.89	152.9	75	14.14	0.04	0.092	77	1364	3814.173	537700	1719.32	5.76
G3.7	527280	8672675	6.68	778.96	6.57	150.39	200	49.5	0.21	0.033	77	1315	3727.271	537300	1737.74	3.43
G3.9	527335	8672826	5.55	790.62	4.96	153.38	1250	259.5	-1.72	0.004	76	1292	3643.423	534900	1751.202	3.42
G3.10	527320	8672919	1.99	798.06	4.8	166.87	175	30	-3.86	0.027	76	1275	3591.076	536300	1763.261	4.05
G3.11	527145	8672780	4.11	790.61	3.7	193.78	600	115	0.2	0.006	76	1292	3643.494	532900	1785.507	2.30
G3.12	527077	8672700	4.93	784.68	3.57	187.34	525	100	0.25	0.007	76	1302	3685.802	532400	1787.133	2.43
G4.1	527629	8672814	6.92	760.11	12.83	135.5	1200	332.34	-4.79	0.011	77	1384	3871.004	541000	1505.581	7.32
G4.2	527674	8673000	3.53	778.42	11.06	128.27	1000	275.77	-2.05	0.011	77	1318	3731.225	537100	1646.277	2.68
G4.3	527628	8673164	4.80	798.04	7.08	116.1	50	7.07	0.17	0.142	76	1275	3591.215	530300	1764.195	10.76
G4.4	527729	8673119	5.90	782.33	10.84	117.11	525	141.42	-1.05	0.021	76	1308	3702.76	531400	1676.558	19.32
G4.5	527845	8673224	5.20	769.05	11.63	107.42	1025	200	0.16	0.011	77	1356	3801.466	524900	1690.591	31.57
G4.6	527755	8673356	1.98	789.52	8.95	104.6	700	135	-6.1	0.013	76	1293	3651.237	525200	1744.878	24.69
G4.7	527634	8673387	3.05	802.25	3.63	58.27	200	49.5	-2.69	0.018	74	1263	3562.311	518800	1843.865	15.37
G4.8	527533	8673301	3.04	805.8	0.47	67.5	375	70	-4.49	0.001	74	1259	3538.077	526300	1845.289	13.11
G4.9	527439	8672989	9.89	799.16	5.03	147	225	56.57	0.23	0.022	74	1266	3583.477	534900	1773.87	6.90
G4.10	527518	8673083	6.74	801.15	4.54	138.5	500	134.35	-1	0.009	74	1263	3569.839	532800	1776.891	5.32
G4.11	527679	8673259	2.51	796.9	7.16	106.71	300	55	-1.02	0.024	76	1278	3599.164	526700	1768.834	2.92

Table II. 2 Diversity indices for Foxfonna ice cap samples.

Sample	Number of OTUs (S)	Pielou's evenness (J')	Shannon Index (H'(Log _e))
G1.1	476	0.64	3.97
G1.2	512	0.74	4.61
G1.3	517	0.72	4.53
G1.4	517	0.79	4.96
G1.5	519	0.73	4.57
G1.6	487	0.70	4.30
G1.7	515	0.75	4.68
G2.1	474	0.70	4.33
G2.2	526	0.76	4.77
G2.3	412	0.65	3.91
G2.4	492	0.74	4.61
G2.5	550	0.76	4.79
G2.6	508	0.73	4.55
G2.7	543	0.72	4.54
G2.8	519	0.73	4.58
G2.9	487	0.70	4.31
G3.1	470	0.72	4.44
G3.2	508	0.70	4.36
G3.3	498	0.67	4.16
G3.5	472	0.59	3.65
G3.6	508	0.72	4.50
G3.7	508	0.71	4.39
G3.9	363	0.67	3.95
G3.10	525	0.75	4.69
G3.11	524	0.77	4.80
G3.12	551	0.77	4.86
G4.1	503	0.64	3.99
G4.2	501	0.76	4.72
G4.3	447	0.76	4.65
G4.4	399	0.72	4.31
G4.5	396	0.69	4.10
G4.6	458	0.76	4.65
G4.7	329	0.68	3.92
G4.8	432	0.69	4.19
G4.9	353	0.67	3.94
G4.10	515	0.78	4.85
G4.11	489	0.78	4.81

Table II. 3 Marginal tests from distLM model of environmental predictors of bacterial community structure. Aspect is in degrees (0 = N, 90 = E). SS: sums of squares; Pseudo-F: test statistic.

Variable	SS(trace)	Pseudo-F	P	Proportion explained
E	2351.7	3.8009	0.001	9.80E-02
N	2276.1	3.6659	0.001	9.48E-02
Chl <i>a</i> ($\mu\text{g}\cdot\text{g}^{-1}$)	1380.4	2.1353	0.012	5.75E-02
Z (m a.s.l.)	1950.3	3.0947	0.002	8.12E-02
Slope (°)	2217.8	3.5625	0.002	9.24E-02
Aspect (°)	1861	2.9412	0.004	7.75E-02
ACCUMAREA (m ²)	705.35	1.0595	0.355	2.94E-02
Flowlength (m)	745.34	1.1214	0.283	3.10E-02
Curvature	623.13	0.93268	0.474	2.60E-02
Wetness	538.76	0.80348	0.633	2.24E-02
PDDs (in summer)	3549	6.0717	0.001	0.14783
PosHrs	1915.8	3.0353	0.003	7.98E-02
PDH	1826.8	2.8827	0.003	7.61E-02
IR (W)	783.44	1.1807	0.238	3.26E-02
IRH (hrs)	1579.3	2.4646	0.003	6.58E-02
ACA (%)	1718.1	2.6979	0.012	7.16E-02

Table II. 4 Sequential tests from distLM model of environmental predictors of bacterial community structure.

Variable	Adj R ²	SS(trace)	Pseudo-F	P	Proportion explained	Cumulative variance
PDDs (in summer)	0.12	3549	6.1	0.001	0.15	0.15
Slope (°)	0.21	2588.5	4.9	0.001	0.11	0.26
N	0.24	1248.6	2.5	0.001	0.05	0.31
ACA (%)	0.27	1005.9	2.1	0.011	0.04	0.35
E	0.31	1372.8	3	0.002	0.06	0.41
Wetness	0.31	503.5	1.1	0.319	0.02	0.43
FAA (m ²)	0.32	517.2	1.1	0.309	0.02	0.45
IR (kW)	0.32	459.1	1	0.399	0.02	0.47
PDH	0.33	661.2	1.5	0.106	0.03	0.5
Z (m a.s.l.)	0.33	511.8	1.1	0.264	0.02	0.5
IR (W)	0.33	0	0	1	0	0.52

Table II. 5 Marginal tests from distLM model of core predictors of tail population structure.

Variable	SS(trace)	Pseudo-F	P	Proportion explained
<i>Leptolyngbya</i> -40205	1737.8	2.5231	0.008	6.72E-02
<i>Microbacteriaceae</i> -32521	3207.3	4.959	0.002	0.1241
<i>Betaproteobacteria</i> -5709	3313.2	5.1468	0.001	0.1282
<i>Gemmatimonadales</i> -59904	2830.6	4.3049	0.001	0.10953
<i>Chloroflexi</i> -37757	3310.7	5.1423	0.001	0.1281
Unassigned-53430	3114.8	4.7963	0.001	0.12052
<i>Sphingomonadaceae</i> -11564	2707.8	4.0963	0.001	0.10477
<i>Intrasporangiaceae</i> -1447	1640.2	2.3719	0.023	6.35E-02
<i>Intrasporangiaceae</i> -46072	2177.5	3.2203	0.004	8.43E-02
<i>Intrasporangiaceae</i> -53638	2178	3.221	0.006	8.43E-02
<i>Intrasporangiaceae</i> -27964	2317.7	3.448	0.004	8.97E-02
<i>Betaproteobacteria</i> -10679	1665.9	2.4115	0.016	6.45E-02
<i>Phormidium</i> -45763	1380.1	1.9744	0.041	5.34E-02
<i>Xanthomonadaceae</i> -51358	1556.4	2.2428	0.016	6.02E-02
<i>Comamonadaceae</i> -22304	1724	2.5017	0.007	6.67E-02
<i>Sphingobacteriaceae</i> -61341	5031.6	8.4615	0.001	0.19469

Table II. 6 Sequential tests from distLM model of core predictors of tail population structure.

Variable	Adj R ²	SS(trace)	Pseudo-F	P	Proportion explained	Cumulative variance
<i>Sphingobacteriaceae</i> -61341	0.17168	5031.6	8.4615	0.001	0.19469	0.19469
<i>Microbacteriaceae</i> -32521	0.2933	3563.1	7.0231	0.001	0.13787	0.33256
<i>Intrasporangiaceae</i> -46072	0.36705	2254.5	4.9617	0.001	8.72E-02	0.41979
<i>Intrasporangiaceae</i> -27964	0.40725	1377.9	3.238	0.001	5.33E-02	0.47311
<i>Leptolyngbya</i> -40205	0.4398	1149.9	2.8594	0.001	4.45E-02	0.5176
<i>Chloroflexi</i> -37757	0.46332	908.77	2.3587	0.001	3.52E-02	0.55277
<i>Phormidium</i> -45763	0.48182	770.48	2.0712	0.001	2.98E-02	0.58258
<i>Intrasporangiaceae</i> -53638	0.49541	645.15	1.781	0.004	2.50E-02	0.60754
<i>Intrasporangiaceae</i> -1447	0.50795	605.33	1.7137	0.004	2.34E-02	0.63097
<i>Gemmatimonadales</i> -59904	0.51475	479.99	1.3779	0.078	1.86E-02	0.64954
<i>Comamonadaceae</i> -22304	0.52067	454.63	1.3212	0.092	1.76E-02	0.66713
<i>Sphingomonadaceae</i> -11564	0.52809	471.93	1.393	0.062	1.83E-02	0.68539
<i>Betaproteobacteria</i> -5709	0.53237	409.6	1.2201	0.189	1.58E-02	0.70124
<i>Xanthomonadaceae</i> -51358	0.53674	404.58	1.2165	0.191	1.57E-02	0.71689
<i>Betaproteobacteria</i> -10679	0.54037	387.33	1.1738	0.258	1.50E-02	0.73188
Unassigned-53430	0.54184	351.13	1.0676	0.359	1.36E-02	0.74547

Table II. 7 Marginal tests from distLM model of environmental and core OTU predictors of total population structure. Aspect is in degrees (0 = N, 90 = E).

Variable	SS(trace)	Pseudo-F	P	Proportion explained
E	2351.7	3.8009	0.001	9.80E-02
N	2276.1	3.6659	0.001	9.48E-02
Chl <i>a</i> (µg.g ⁻¹)	1380.4	2.1353	0.024	5.75E-02
Z (m a.s.l.)	1950.3	3.0947	0.001	8.12E-02
Slope (°)	2217.8	3.5625	0.001	9.24E-02
Aspect (°)	1861	2.9412	0.004	7.75E-02
ACCUMAREA (m ²)	705.35	1.0595	0.326	2.94E-02
Flowlength (m)	745.34	1.1214	0.282	3.10E-02
Curvature	623.13	0.93268	0.469	2.60E-02
Wetness	538.76	0.80348	0.625	2.24E-02
PDDs (in summer)	3549	6.0717	0.001	0.14783
PosHrs	1915.8	3.0353	0.002	7.98E-02
PDH	1826.8	2.8827	0.002	7.61E-02
IR (W)	783.44	1.1807	0.264	3.26E-02
IRH (hrs)	1579.3	2.4646	0.009	6.58E-02
IR (kW)	783.44	1.1807	0.241	3.26E-02
ACA (%)	1718.1	2.6979	0.008	7.16E-02
<i>Leptolyngbya</i> -40205	1668.1	2.6136	0.01	6.95E-02
<i>Microbacteriaceae</i> -32521	3044.6	5.0834	0.001	1.27E-01
<i>Betaproteobacteria</i> -5709	3160.5	5.3062	0.001	1.32E-01
<i>Gemmatimonadales</i> -59904	2753.4	4.5343	0.001	1.15E-01
<i>Chloroflexi</i> -37757	3143.9	5.2743	0.001	1.31E-01
Unassigned-53430	2933.2	4.8715	0.001	1.22E-01
<i>Sphingomonadaceae</i> -11564	2598.9	4.249	0.001	1.08E-01
<i>Intrasporangiaceae</i> -1447	1571.9	2.4522	0.021	6.55E-02
<i>Intrasporangiaceae</i> -46072	2076.3	3.3136	0.004	8.65E-02
<i>Intrasporangiaceae</i> -53638	2071.3	3.3048	0.004	8.63E-02
<i>Betaproteobacteria</i> -10679	1613.6	2.522	0.011	6.72E-02
<i>Intrasporangiaceae</i> -27964	2217.5	3.5619	0.003	9.24E-02
<i>Phormidium</i> -45763	1308	2.0169	0.049	5.45E-02
<i>Xanthomonadaceae</i> -51358	1449.9	2.2497	0.016	6.04E-02
<i>Sphingobacteriaceae</i> -61341	4724	8.5744	0.001	1.97E-01
<i>Comamonadaceae</i> -22304	1621	2.5344	0.009	6.75E-02

Table II. 8 Sequential tests of distLM model of environmental and core OTU predictors of total community structure.

Variable	Adj R ²	SS(trace)	Pseudo-F	P	Proportion explained	Cumulative variance
<i>Sphingobacteriaceae</i> -61341	0.17383	4724	8.5744	0.001	0.19678	0.19678
<i>Microbacteriaceae</i> -32521	0.30011	3414.2	7.3152	0.001	0.14222	0.33899
<i>Intrasporangiaceae</i> -46072	0.37552	2126.3	5.1058	0.001	8.86E-02	0.42756
<i>Intrasporangiaceae</i> -27964	0.41655	1292	3.3206	0.001	5.38E-02	0.48138
<i>Leptolyngbya</i> -40205	0.45091	1099.3	3.002	0.001	4.58E-02	0.52717
<i>Chloroflexi</i> -37757	0.47495	847.14	2.4195	0.001	3.53E-02	0.56246
Unassigned-53430	0.49359	710.75	2.1046	0.001	2.96E-02	0.59206
<i>Phormidium</i> -45763	0.50765	600.2	1.828	0.006	2.50E-02	0.61706
E	0.52116	571.54	1.7899	0.005	2.38E-02	0.64087
N	0.53297	524.02	1.6825	0.012	2.18E-02	0.6627
<i>Intrasporangiaceae</i> -1447	0.54173	457.47	1.4969	0.026	1.91E-02	0.68175
Z (m a.s.l.)	0.5477	401.21	1.3302	0.091	1.67E-02	0.69847
<i>Betaproteobacteria</i> -5709	0.55606	429.91	1.4522	0.049	1.79E-02	0.71637
<i>Gemmatimonadales</i> -59904	0.56188	381.44	1.3056	0.123	1.59E-02	0.73226
IRH (hrs)	0.56673	359.99	1.2459	0.193	1.50E-02	0.74726
IR (kW)	0.57324	375.79	1.3205	0.118	1.57E-02	0.76291
<i>Xanthomonadaceae</i> -51358	0.57896	357.06	1.2717	0.16	1.49E-02	0.77778
<i>Betaproteobacteria</i> -10679	0.58411	342.55	1.2351	0.221	1.43E-02	0.79205
PDH	0.58719	312.35	1.1347	0.336	1.30E-02	0.80506
<i>Sphingomonadaceae</i> -11564	0.59007	305.95	1.1192	0.321	1.27E-02	0.81781
Wetness	0.5921	293.73	1.0798	0.356	1.22E-02	0.83004
<i>Intrasporangiaceae</i> -53638	0.59372	287.07	1.0596	0.39	1.20E-02	0.842
ACA (%)	0.59631	293.43	1.09	0.372	1.22E-02	0.85422
PDDs (in summer)	0.60088	305.78	1.1489	0.356	1.27E-02	0.86696
Curvature	0.60456	293.12	1.1115	0.365	1.22E-02	0.87917

Table II. 9 Sequential tests of distLM model of environmental and core OTU predictors of tail community structure.

Variable	Adj R ²	SS(trace)	Pseudo-F	P	Proportion explained	Cumulative variance
<i>Sphingobacteriaceae</i> -61341	0.17	4985.8	8.36	0.001	0.19	0.19
<i>Microbacteriaceae</i> -32521	0.292	3584.5	7.05	0.001	0.14	0.33
<i>Intrasporangiaceae</i> -46072	0.367	2287.7	5.03	0.001	0.09	0.42
<i>Intrasporangiaceae</i> -27964	0.408	1389.6	3.27	0.001	0.05	0.47
<i>Leptolyngbya</i> -40205	0.441	1172.5	2.92	0.001	0.05	0.52
<i>Chloroflexi</i> -37757	0.464	884.78	2.3	0.001	0.03	0.55
<i>Phormidium</i> -45763	0.483	791.69	2.13	0.001	0.03	0.58
N	0.5	700.72	1.95	0.002	0.03	0.61
E	0.513	623.48	1.78	0.005	0.02	0.63
<i>Intrasporangiaceae</i> -1447	0.523	526.4	1.53	0.022	0.02	0.66
IRH (hrs)	0.531	496.06	1.47	0.036	0.02	0.67
Unassigned-53430	0.537	441.15	1.33	0.09	0.02	0.69
PDH	0.542	414.92	1.26	0.168	0.02	0.71
<i>Betaproteobacteria</i> -5709	0.551	466.38	1.45	0.05	0.02	0.73
<i>Gemmatimonadales</i> -59904	0.556	408.67	1.28	0.165	0.02	0.74
IR (kW)	0.561	383.75	1.22	0.202	0.01	0.76
<i>Xanthomonadaceae</i> -51358	0.566	379.77	1.22	0.208	0.01	0.77
Z (m a.s.l.)	0.571	379.05	1.23	0.208	0.01	0.79
<i>Betaproteobacteria</i> -10679	0.574	346.03	1.13	0.328	0.01	0.8
Wetness	0.576	334.33	1.1	0.344	0.01	0.81
<i>Sphingomonadaceae</i> -11564	0.577	313.92	1.03	0.421	0.01	0.82
<i>Intrasporangiaceae</i> -53638	0.581	341.19	1.13	0.342	0.01	0.84
ACA (%)	0.582	312.92	1.04	0.443	0.01	0.85
PDDs (in summer)	0.587	344.06	1.16	0.324	0.01	0.86
Curvature	0.592	328.7	1.12	0.36	0.01	0.88
Chl <i>a</i> (µg.g ⁻¹)	0.592	296.43	1.01	0.45	0.01	0.89
PosHrs	0.593	298.39	1.02	0.438	0.01	0.9
<i>Betaproteobacteria</i> -5709	0.593	291.84	1	0.474	0.01	0.89

Table II. 10 Marginal tests from distLM model of environmental and core OTU predictors of tail population structure. Aspect is in degrees (0 = N, 90 = E).

Variable	SS(trace)	Pseudo-F	P	Proportion explained
E	2472.3	3.6988	0.001	0.1
N	2445.5	3.65E+00	0.001	0.09
Chl <i>a</i> (µg.g ⁻¹)	1499.8	2.15E+00	0.021	0.06
Z (m a.s.l.)	2101.1	3.09E+00	0.002	0.08
Slope (°)	2369	3.53E+00	0.001	0.09
Aspect (°)	1969.2	2.88E+00	0.001	0.08
ACCUMAREA (m ²)	769.03	1.07E+00	0.318	0.03
Flowlength (m)	812.22	1.13E+00	0.289	0.03
Curvature	668.69	9.29E-01	0.477	0.03
Wetness	599.19	8.30E-01	0.59	0.02
PDDs (in summer)	3771.8	5.97E+00	0.001	0.15
PosHrs	2064.1	3.04E+00	0.002	0.08
PDH	1969.8	2.89E+00	0.003	0.08
IR (W)	825.09	1.15E+00	0.25	0.03
IRH (hrs)	1654.7	2.39E+00	0.008	0.06
IR (kW)	825.09	1.15E+00	0.275	0.03
ACA (%)	1802.4	2.62E+00	0.007	0.07
<i>Leptolyngbya</i> -40205	1809	2.6319	0.008	0.07
<i>Microbacteriaceae</i> -32521	3228	4.99E+00	0.001	0.12479
<i>Betaproteobacteria</i> -5709	3288	5.10E+00	0.001	0.12712
<i>Gemmatimonadales</i> -59904	2803.4	4.25E+00	0.001	0.10838
<i>Chloroflexi</i> -37757	3354	5.21E+00	0.001	0.12967
Unassigned-53430	3136.9	4.83E+00	0.001	0.12127
<i>Sphingomonadaceae</i> -11564	2850.5	4.33E+00	0.001	0.1102
<i>Intrasporangiaceae</i> -1447	1672.1	2.42E+00	0.019	6.46E-02
<i>Intrasporangiaceae</i> -46072	2197.4	3.25E+00	0.005	8.50E-02
<i>Intrasporangiaceae</i> -53638	2191.5	3.24E+00	0.006	8.47E-02
<i>Intrasporangiaceae</i> -27964	2328.9	3.46E+00	0.004	9.00E-02
<i>Betaproteobacteria</i> -10679	1639.1	2.368	0.016	6.34E-02
<i>Phormidium</i> -45763	1390.3	1.99E+00	0.042	5.38E-02
<i>Xanthomonadaceae</i> -51358	1559.1	2.2449	0.006	6.03E-02
<i>Comamonadaceae</i> -22304	1729.1	2.51E+00	0.007	6.68E-02
<i>Sphingobacteriaceae</i> -61341	4985.8	8.36E+00	0.001	0.19275

APPENDIX III

Supplementary Tables and Figures for “Chapter 5 - Biotic and abiotic influence on the metabolomic profile of High Arctic ice cap cryoconite on Foxfonna, Svalbard”.

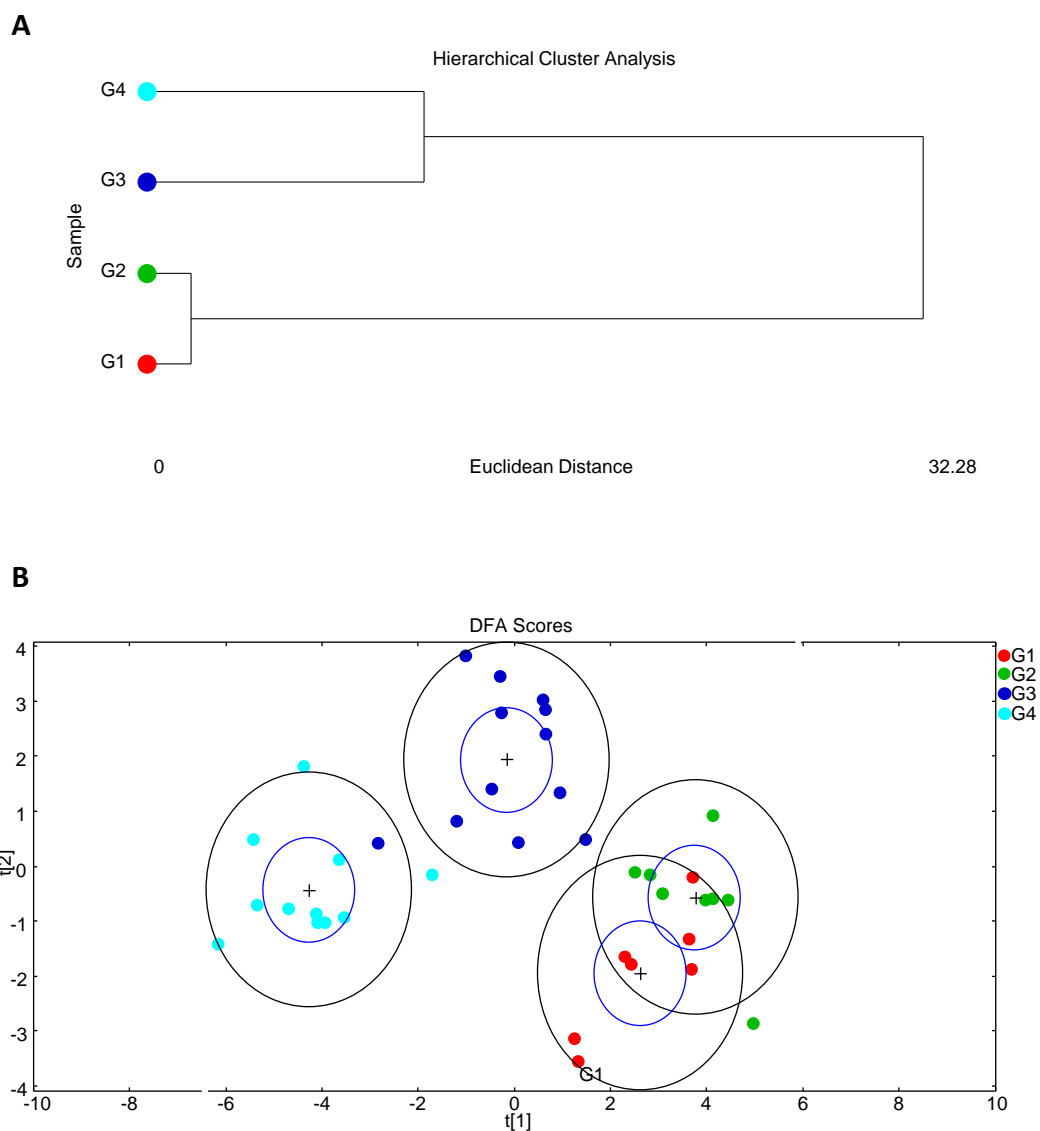


Figure III. 1 Multivariate analysis of Foxfonna ice cap metabolites by both (A) hierarchical cluster analysis and (B) detrended fluctuation analysis show the distinct natural clustering patterns of the metabolite separate sectors G1 and G2 from sectors G3 and G4 along a geographical demarcation point.

Table III. 1 Tentative metabolite ID of importance established by post hoc ANOVA ($P < 0.05$) filtering on Metaboanalyst 3.0.

Tentative Metabolite ID	F value	P value	False Discovery Rate
2-oxobutanoate	78.421	1.32E-15	9.22E-14
Ferulic acid	41.021	1.49E-11	5.22E-10
Homoglutamine	23.211	1.89E-08	4.42E-07
Gluconic acid	19.898	1.06E-07	1.85E-06
Syringic acid	18.379	2.48E-07	3.47E-06
Dihydroorotate	16.847	6.10E-07	7.11E-06
GABA	15.715	1.22E-06	1.22E-05
Erythrose-4-phosphate	13.738	4.41E-06	3.86E-05
Glucosaminic acid	12.652	9.32E-06	7.25E-05
3-4-dihydroxy-L-phenylalanine	11.485	2.16E-05	0.000151
Maltose	11.017	3.05E-05	0.000194
R-S-lactoylglutathione	10.87	3.41E-05	0.000199
Riboflavin	10.647	4.04E-05	0.000218
Jasmonic acid	10.259	5.44E-05	0.000272
Tyrosine	9.9445	6.96E-05	0.000312
2',3'-cyclic GMP	9.9115	7.14E-05	0.000312
Adenosine	9.3311	0.00011338	0.000467
Stearic acid	8.8992	0.00016121	0.000627
Urate	8.2515	0.00027684	0.00102
Pelargonidin	8.0696	0.00032316	0.001131
N-acetyl-L-glutamate-5-phosphate	7.8712	0.00038318	0.001277
Naringenin	7.7082	0.00044125	0.001404
5'-methylthioadenosine	7.5222	0.00051901	0.00158
O-acetyl-L-homoserine	6.4453	0.0013671	0.003988
Flavin mononucleotide	6.1148	0.0018593	0.005204
3',5'-cyclic dAMP	6.0735	0.0019328	0.005204
Docosaheptaenoic acid	6.0066	0.0020586	0.005337
Fucoxanthin	5.9402	0.0021916	0.005479
Ribulose-5-phosphate	5.8159	0.0024661	0.005953
Linolenic acid	5.4239	0.0035943	0.008387
Catechin	5.2454	0.0042773	0.009658
Coniferyl aldehyde	5.0501	0.0051831	0.011338
sn-glycerol-3-phosphate	4.9979	0.0054578	0.011577
Oxaloacetate	4.8692	0.0062024	0.01277
Proline	4.7431	0.0070366	0.014073
Neoxanthin	4.709	0.0072812	0.014158
Myricetin	4.662	0.0076339	0.014371
Inosine	4.6216	0.0079516	0.014371
Cystathionine	4.6147	0.0080067	0.014371
Xanthosine-5'-phosphate	4.5677	0.0083967	0.014694
Adenine	4.5263	0.0087567	0.01474
Arachidonic acid	4.5165	0.008844	0.01474
Thymidine	4.49	0.0090853	0.01479
Fumarate	4.4447	0.0095135	0.015135

Table III. 1 Tentative metabolite ID of importance established by post hoc ANOVA ($P < 0.05$) filtering on Metaboanalyst 3.0. (continued)

Tentative Metabolite ID	F value	P value	False Discovery Rate
Citric acid	4.2744	0.011323	0.017613
ATP	4.1627	0.012702	0.019328
Kaempferol	4.1223	0.013243	0.019724
Serine	4.0452	0.014345	0.02092
Cytosine	3.8768	0.017096	0.024423
Fructose-1,6-bisphosphate	3.8261	0.01803	0.025241
Spermine	3.8005	0.01852	0.02542
Oleic acid	3.7741	0.01904	0.02563
Cysteine	3.6846	0.020924	0.027635
Linoleic acid	3.6591	0.021494	0.027862
Pyrophosphate	3.5952	0.022998	0.029271
O-succinyl-L-homoserine	3.5381	0.024436	0.030545
Indole-3-glycerol-phosphate	3.4821	0.025935	0.03185
Glucosamine	3.4454	0.02697	0.03244
Hexose-phosphate	3.4326	0.027342	0.03244
Xanthoxin	3.4049	0.028163	0.032856
Antheraxanthin	3.2694	0.032569	0.037374
Palmitic acid	3.2169	0.034463	0.03891
Sphinganine-1-phosphate	3.2	0.035097	0.038997
Mannitol	3.1788	0.035909	0.039231
2',3'-cyclic AMP	3.1655	0.036428	0.039231
GTP	3.1228	0.03815	0.040462
Asparagine	3.0828	0.039841	0.041617
Alpha-carotene	3.0693	0.040428	0.041617
5-HPETE	3.0328	0.042063	0.042672
Sinapaldehyde	3.0163	0.042824	0.042824

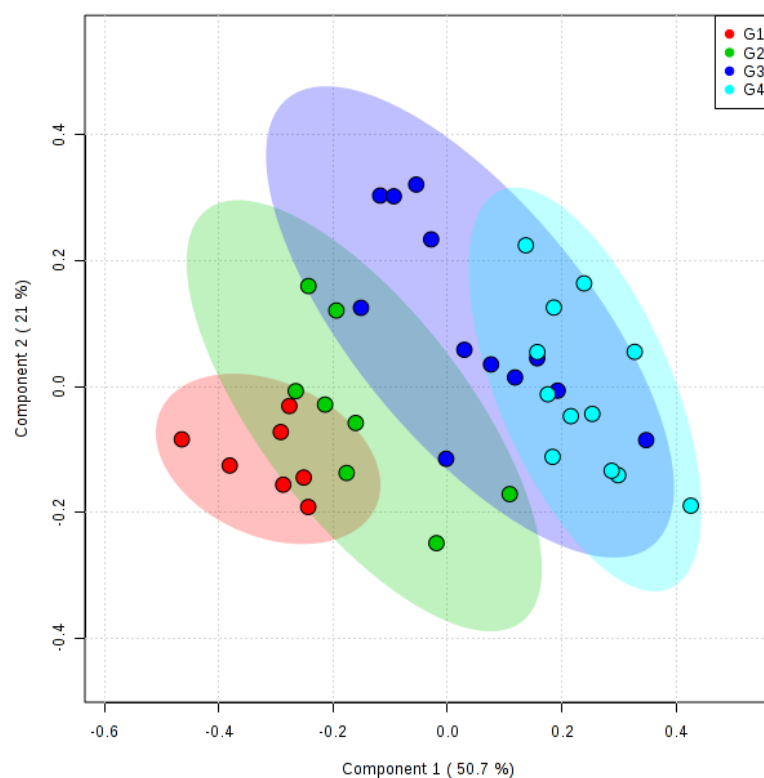


Figure III. 2 TCA cycle metabolites represented in partial least squares discriminant analysis (PLS-DA), with clear sector influence on the metabolite clustering pattern.

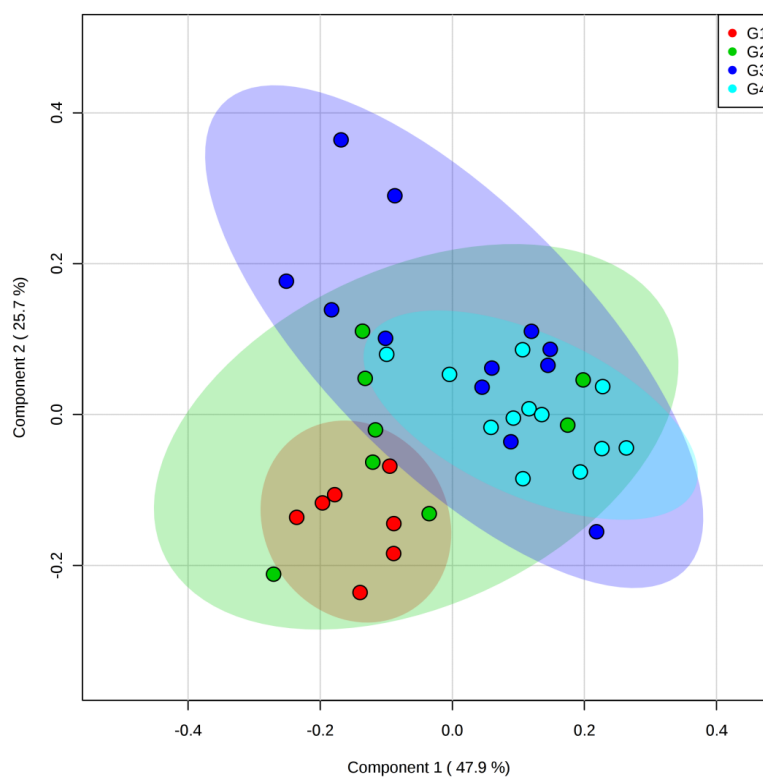


Figure III. 3 PLS-DA of polyamine metabolites show discrete metabolite clustering for each sector, with sector G1 separating into an isolated cluster.

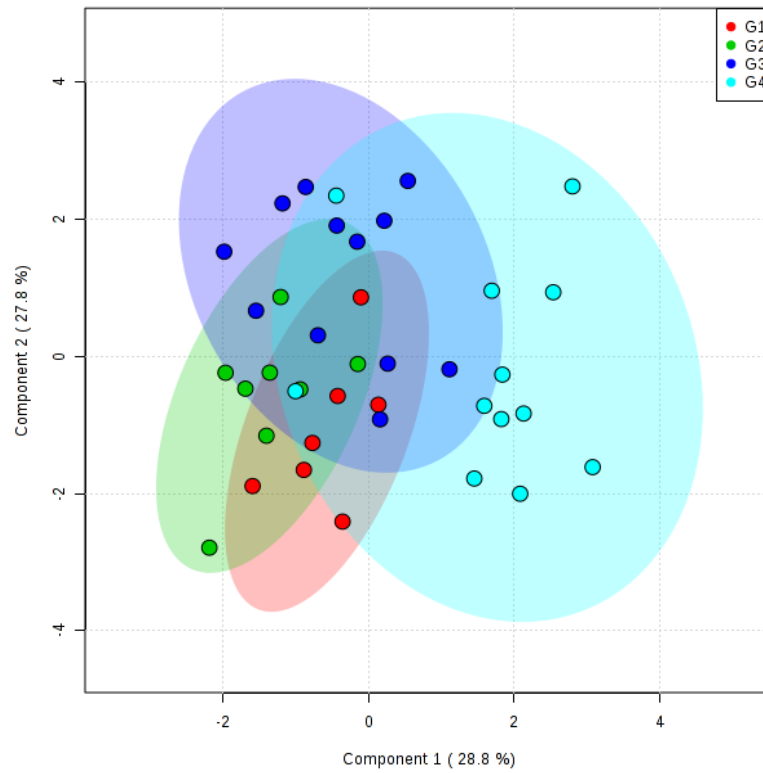


Figure III. 4 Lipid metabolite profile of ice cap cryoconite shows clustering by sector in PLS-DA, with sector G4 separating out from the other 3 sectors.

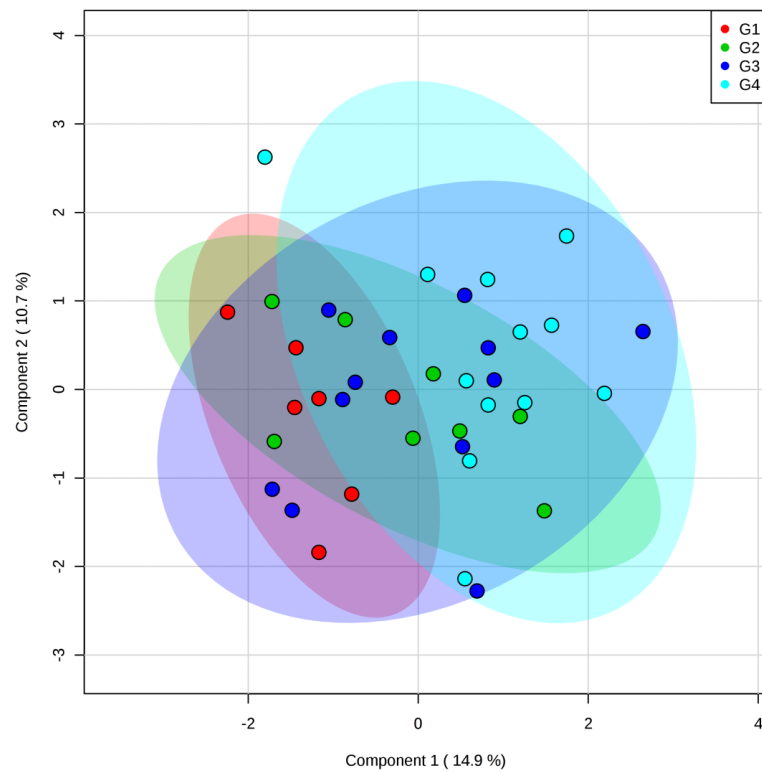


Figure III. 5 There is an absence of separation in the PLS-DA for photosynthesis metabolites across the entire dome in the 95% confidence interval, with a minimal sector-bias effect.

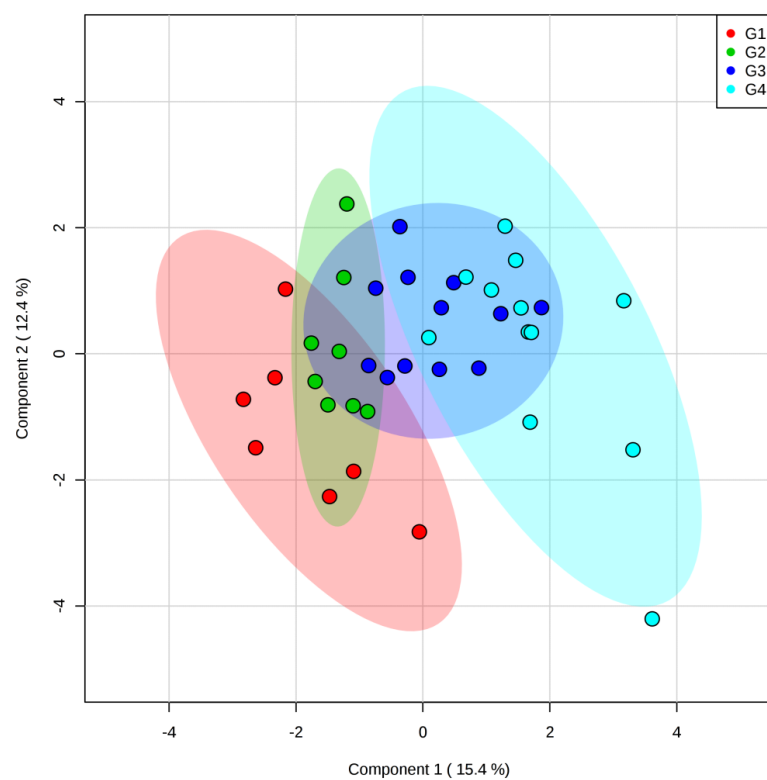


Figure III. 6 Nucleic acid metabolites show a strong sector-based east-west pattern of separation, with discrete clustering within each sector.

Table III. 2 Marginal tests of core taxa, keystone taxa and environmental parameters in redundancy analysis of total metabolites. Aspect is in degrees (0 = N, 90 = E).

Variable	SS(trace)	Pseudo-F	P	Proportion explained
E	4.062	12.721	0.001	0.27227
N	0.96025	2.3389	0.043	6.44E-02
Chl <i>a</i> (µg.g ⁻¹)	0.91475	2.2208	0.061	6.13E-02
Z (m a.s.l)	2.7508	7.6861	0.001	0.18438
Slope	0.32971	0.76837	0.565	2.21E-02
Aspect (°)	2.0849	5.5233	0.002	0.13975
FAA	1.2423	3.0884	0.021	8.33E-02
Flowlength	1.2694	3.1619	0.023	8.51E-02
Curvature	0.51477	1.215	0.257	3.45E-02
Wetness	0.28162	0.65415	0.61	1.89E-02
PDDs	2.115	5.6162	0.001	0.14177
PosHrs	2.8478	8.0212	0.001	0.19088
PDH	2.7162	7.5679	0.002	0.18206
IR (W)	2.0253	5.3406	0.002	0.13575
IRH (hrs)	0.6513	1.552	0.151	4.37E-02
IR (kW)	2.0253	5.3406	0.001	0.13575
ACA (%)	0.61076	1.4513	0.196	4.09E-02
<i>O. tianjinense</i> -53638	1.2475	3.1024	0.033	8.36E-02
<i>H. albus</i> -27964	1.341	3.3579	0.028	8.99E-02
<i>Iamia</i> -61555	1.1912	2.9501	0.035	7.98E-02
<i>Azospirillum</i> -37757	0.84626	2.0446	0.067	5.67E-02
<i>Eubacterium</i> -1447	0.44452	1.0441	0.356	2.98E-02
Ellin5220-51679	0.45973	1.081	0.34	3.08E-02
<i>Rhizobium</i> -53430	0.79849	1.9226	0.089	5.35E-02
Ellin7143-48894	0.13981	0.32164	0.926	9.37E-03
<i>P. priestleyi</i> -40205	0.59489	1.412	0.195	3.99E-02
<i>Frigoribacterium</i> -32521	0.65665	1.5654	0.155	4.40E-02
<i>Massilia</i> -5709	0.7295	1.748	0.11	4.89E-02
Ellin5220-59904	1.9105	4.9933	0.001	0.12806
<i>Novosphingobium</i> -11564	0.17951	0.41406	0.889	1.20E-02
<i>Oryzihumus</i> -46072	0.40736	0.95441	0.403	2.73E-02
<i>T. mixta</i> -10679	1.5161	3.846	0.015	0.10162
<i>Arsenicicoccus</i> -41255	1.2565	3.1269	0.025	8.42E-02
<i>P. daechungensis</i> -61341	1.4666	3.7066	0.01	9.83E-02
<i>P. autumnale</i> -45763	0.53015	1.2527	0.224	3.55E-02
<i>P. sacheonensis</i> -51358	0.42883	1.0062	0.409	2.87E-02
<i>Curvibacter</i> -22304	0.71958	1.723	0.124	4.82E-02

Table III. 3 Sequential tests of core taxa, keystone taxa and environmental parameters in redundancy analysis of total metabolites. Aspect is in degrees (0 = N, 90 = E).

Variable	R ²	SS(trace)	Pseudo-F	P	Proportion explained	Cumulative variance
E	0.27227	4.062	12.721	0.001	0.27227	0.27227
N	0.35699	1.264	4.3482	0.001	8.47E-02	0.35699
PDDs	0.42278	0.98143	3.6469	0.008	6.58E-02	0.42278
Chl <i>a</i> (µg.g ⁻¹)	0.46117	0.57279	2.2088	0.033	3.84E-02	0.46117
<i>Novosphingobium</i> -11564	0.6549	0.41633	1.8598	0.056	2.79E-02	0.6549
IRH (hrs)	0.84165	0.4329	2.3822	0.057	2.90E-02	0.84165
Ellin5220-59904	0.89	0.33764	2.263	0.077	2.26E-02	0.89
<i>Massilia</i> -5709	0.49017	0.43268	1.7065	0.09	2.90E-02	0.49017
<i>Eubacterium</i> -1447	0.56796	0.39378	1.6495	0.11	2.64E-02	0.56796
Ellin5220-51679	0.9084	0.27457	2.0091	0.113	1.84E-02	0.9084
Aspect (°)	0.51627	0.38945	1.565	0.118	2.61E-02	0.51627
<i>P. priestleyi</i> -40205	0.54156	0.3773	1.5446	0.128	2.53E-02	0.54156
<i>Iamia</i> -61555	0.95299	0.23322	1.9951	0.133	1.56E-02	0.95299
FAA	0.76487	0.33053	1.6018	0.145	2.22E-02	0.76487
<i>O. tianjinense</i> -53638	0.74272	0.34034	1.596	0.153	2.28E-02	0.74272
Z	0.99765	0.17174	4.9011	0.189	1.15E-02	0.99765
<i>P. daechungensis</i> -61341	0.60961	0.30927	1.3275	0.201	2.07E-02	0.60961
<i>Curvibacter</i> -22304	0.58888	0.31216	1.3232	0.223	2.09E-02	0.58888
Slope	0.81264	0.25743	1.2893	0.254	1.73E-02	0.81264
ACA	0.67304	0.27061	1.2205	0.275	1.81E-02	0.67304
<i>H. albus</i> -27964	0.97164	0.15243	1.4411	0.294	1.02E-02	0.97164
PosHrs	0.79538	0.25426	1.2493	0.294	1.70E-02	0.79538
<i>Oryzihumus</i> -46072	0.92751	0.17609	1.3026	0.299	1.18E-02	0.92751
<i>Rhizobium</i> -53430	0.68979	0.24992	1.134	0.333	1.68E-02	0.68979
Curvature	0.9806	0.13363	1.385	0.336	8.96E-03	0.9806
<i>Frigoribacterium</i> -32521	0.62699	0.25935	1.1185	0.349	1.74E-02	0.62699
Wetness	0.71991	0.24141	1.0976	0.35	1.62E-02	0.71991
<i>P. autumnale</i> -45763	0.93736	0.14694	1.1006	0.373	9.85E-03	0.93736
<i>Azospirillum</i> -37757	0.96143	0.12586	1.0934	0.385	8.44E-03	0.96143
Ellin7143-48894	0.77834	0.20091	0.97202	0.429	1.35E-02	0.77834
<i>P. sacheonensis</i> -51358	0.70373	0.2079	0.94069	0.482	1.39E-02	0.70373
IR (W)	0.98614	8.27E-02	0.79967	0.5	5.54E-03	0.98614
Flowlength	0.91571	0.109	0.78002	0.521	7.31E-03	0.91571
IR (kW)	0.99765	8.98E-14	0	1	6.02E-15	0.99765

APPENDIX IV

Supplementary Tables and Figures for “Chapter 6 - Bacterial community dynamics of High Arctic valley glacier cryoconite in Foxfonna, Svalbard”.

Table IV. 1 Environmental parameters recorded on Foxfonna valley glacier. Aspect degrees (0 = N, 90 = E).

Sample	Northings (UTM)	Eastings (UTM)	Z (m a.s.l.)	Slope (°)	Aspect (°)	Curvature	FAA (m ²)	Total IR (hrs)	IR between DOY (hrs)
202.FL2C2	8674833.0	525774.3	493.7	7.1	308	0.225	262.9	971	971
202.FL2C5	8674821.0	525770.3	493.9	7.5	297	0.657	78.0	971	971
202.FL4C1	8674373.0	526421.0	597.5	3.4	302	-0.042	615.2	971	971
202.FL4C3	8674369.0	526434.9	598.2	3.5	297	-0.053	529.6	971	971
202.FL4C4	8674364.0	526445.7	598.9	3.5	294	-0.003	474.2	971	971
202.FL4C5	8674351.0	526458.5	599.9	2.6	295	0.192	392.8	971	971
202.FLC1A	8675315.0	525402.8	406.2	13.0	347	-0.151	3071.4	971	971
202.FLC1B	8675315.0	525402.8	406.2	13.0	347	-0.151	3071.4	971	971
202.FLC3A	8674974.0	525694.8	474.6	6.9	322	0.154	515.5	971	971
202.FLC4A	8674867.0	525793.9	492.8	7.4	314	0.238	371.5	971	971
202.FLC8A	8674357.0	526473.3	600.3	2.7	292	-0.188	383.1	971	971
210.FL2C1	8674848.0	525783.6	493.5	7.2	309	0.155	882.8	1149	178
210.FL2C1A	8674848.0	525783.6	493.5	7.2	309	0.155	882.8	1149	178
210.FL2C2	8674833.0	525774.3	493.7	7.1	308	0.225	262.9	1148	177
210.FL2C3	8674836.0	525769.3	492.8	7.3	306	0.093	302.1	1148	177
210.FL2C4	8674820.0	525778.4	495.3	6.6	299	0.496	102.4	1147	176
210.FL2C5	8674821.0	525770.3	493.9	7.5	297	0.657	78.0	1146	175
210.FL4C2	8674373.0	526421.0	597.5	3.4	302	-0.042	615.2	1149	178
210.FLC1A	8675315.0	525402.8	406.2	13.0	347	-0.151	3071.4	1149	178
210.FLC2A	8675108.0	525559.6	450.2	8.6	344	-0.208	1503.0	1149	178
210.FLC3B	8674974.0	525694.8	474.6	6.9	322	0.154	515.5	1149	178
210.FLC4A	8674867.0	525793.9	492.8	7.4	314	0.238	371.5	1149	178
210.FLC4B	8674867.0	525793.9	492.8	7.4	314	0.238	371.5	1149	178
210.FLC5A	8674736.0	525966.2	526.2	9.6	314	0.110	593.3	1149	178
210.FLC5B	8674736.0	525966.2	526.2	9.6	314	0.110	593.3	1149	178
210.FLC8A	8674357.0	526473.3	600.3	2.7	292	-0.188	383.1	1149	178
217.FL2C1	8674848.0	525783.6	493.5	7.2	309	0.155	882.8	1304	1126
217.FL2C2	8674833.0	525774.3	493.7	7.1	308	0.225	262.9	1296	1120
217.FL2C3	8674836.0	525769.3	492.8	7.3	306	0.093	302.1	1295	1119
217.FL2C5	8674821.0	525770.3	493.9	7.5	297	0.657	78.0	1291	1117
217.FL4C1	8674373.0	526421.0	597.5	3.4	302	-0.042	615.2	1310	1132
217.FL4C1A	8674373.0	526421.0	597.5	3.4	302	-0.042	615.2	1310	1132
217.FL4C4	8674364.0	526445.7	598.9	3.5	294	-0.003	474.2	1310	1132
217.FLC2A	8675108.0	525559.6	450.2	8.6	344	-0.208	1503.0	1305	1127
217.FLC2B	8675108.0	525559.6	450.2	8.6	344	-0.208	1503.0	1305	1127
217.FLC4B	8674867.0	525793.9	492.8	7.4	314	0.238	371.5	1310	1132
217.FLC5A	8674736.0	525966.2	526.2	9.6	314	0.110	593.3	1310	1132
217.FLC5B	8674736.0	525966.2	526.2	9.6	314	0.110	593.3	1310	1132

Table IV. 1 Environmental parameters recorded on Foxfonna valley glacier. Aspect in degrees (0 = N, 90 = E) (continued).

Sample	Northings (UTM)	Eastings (UTM)	Z (m a.s.l.)	Slope (°)	Aspect (°)	Curvature	FAA (m ²)	Total IR (hrs)	IR between DOY (hrs)
217.FLC7A	8674487.0	526283.4	580.6	6.9	328	-0.152	2372.3	1310	1132
217.FLC7B	8674487.0	526283.4	580.6	6.9	328	-0.152	2372.3	1310	1132
217.FLC8B	8674357.0	526473.3	600.3	2.7	292	-0.188	383.1	1310	1132
221.FL2C1	8674848.0	525783.6	493.5	7.2	309	0.155	882.8	1389	263
221.FL2C3	8674836.0	525769.3	492.8	7.3	306	0.093	302.1	1378	259
221.FL4C1	8674373.0	526421.0	597.5	3.4	302	-0.042	615.2	1405	273
221.FL4C1A	8674373.0	526421.0	597.5	3.4	302	-0.042	615.2	1405	273
221.FL4C3	8674369.0	526434.9	598.2	3.5	297	-0.053	529.6	1405	273
221.FL4C4	8674364.0	526445.7	598.9	3.5	294	-0.003	474.2	1405	273
221.FL4C5	8674351.0	526458.5	599.9	2.6	295	0.192	392.8	1405	273
221.FLC1A	8675315.0	525402.8	406.2	13.0	347	-0.151	3071.4	1393	262
221.FLC2A	8675108.0	525559.6	450.2	8.6	344	-0.208	1503.0	1390	262
221.FLC3A	8674974.0	525694.8	474.6	6.9	322	0.154	515.5	1391	266
221.FLC4A	8674867.0	525793.9	492.8	7.4	314	0.238	371.5	1398	267
221.FLC4B	8674867.0	525793.9	492.8	7.4	314	0.238	371.5	1398	267
221.FLC5A	8674736.0	525966.2	526.2	9.6	314	0.110	593.3	1405	273
221.FLC5B	8674736.0	525966.2	526.2	9.6	314	0.110	593.3	1405	273
221.FLC7A	8674487.0	526283.4	580.6	6.9	328	-0.152	2372.3	1405	273
221.FLC8A	8674357.0	526473.3	600.3	2.7	292	-0.188	383.1	1405	273
221.FLC8B	8674357.0	526473.3	600.3	2.7	292	-0.188	383.1	1405	273
228.FL2C1	8674848.0	525783.6	493.5	7.2	309	0.155	882.8	1527	1264
228.FL2C2	8674833.0	525774.3	493.7	7.1	308	0.225	262.9	1515	1255
228.FL2C3	8674836.0	525769.3	492.8	7.3	306	0.093	302.1	1513	1254
228.FL2C4	8674820.0	525778.4	495.3	6.6	299	0.496	102.4	1511	1253
228.FL2C5	8674821.0	525770.3	493.9	7.5	297	0.657	78.0	1506	1250
228.FL4C1	8674373.0	526421.0	597.5	3.4	302	-0.042	615.2	1566	1293
228.FL4C2	8674373.0	526421.0	597.5	3.4	302	-0.042	615.2	1566	1293
228.FL4C3	8674369.0	526434.9	598.2	3.5	297	-0.053	529.6	1566	1293
228.FL4C4	8674364.0	526445.7	598.9	3.5	294	-0.003	474.2	1566	1293
228.FL4C5	8674351.0	526458.5	599.9	2.6	295	0.192	392.8	1566	1293
228.FLC1A	8675315.0	525402.8	406.2	13.0	347	-0.151	3071.4	1510	1248
228.FLC1B	8675315.0	525402.8	406.2	13.0	347	-0.151	3071.4	1510	1248
228.FLC3A	8674974.0	525694.8	474.6	6.9	322	0.154	515.5	1531	1265
228.FLC4A	8674867.0	525793.9	492.8	7.4	314	0.238	371.5	1540	1274
228.FLC4B	8674867.0	525793.9	492.8	7.4	314	0.238	371.5	1540	1274
228.FLC5A	8674736.0	525966.2	526.2	9.6	314	0.110	593.3	1566	1293
228.FLC5B	8674736.0	525966.2	526.2	9.6	314	0.110	593.3	1566	1293
228.FLC7A	8674487.0	526283.4	580.6	6.9	328	-0.152	2372.3	1566	1293
228.FLC7B	8674487.0	526283.4	580.6	6.9	328	-0.152	2372.3	1566	1293
228.FLC8A	8674357.0	526473.3	600.3	2.7	292	-0.188	383.1	1566	1293
228.FLC8B	8674357.0	526473.3	600.3	2.7	292	-0.188	383.1	1566	1293

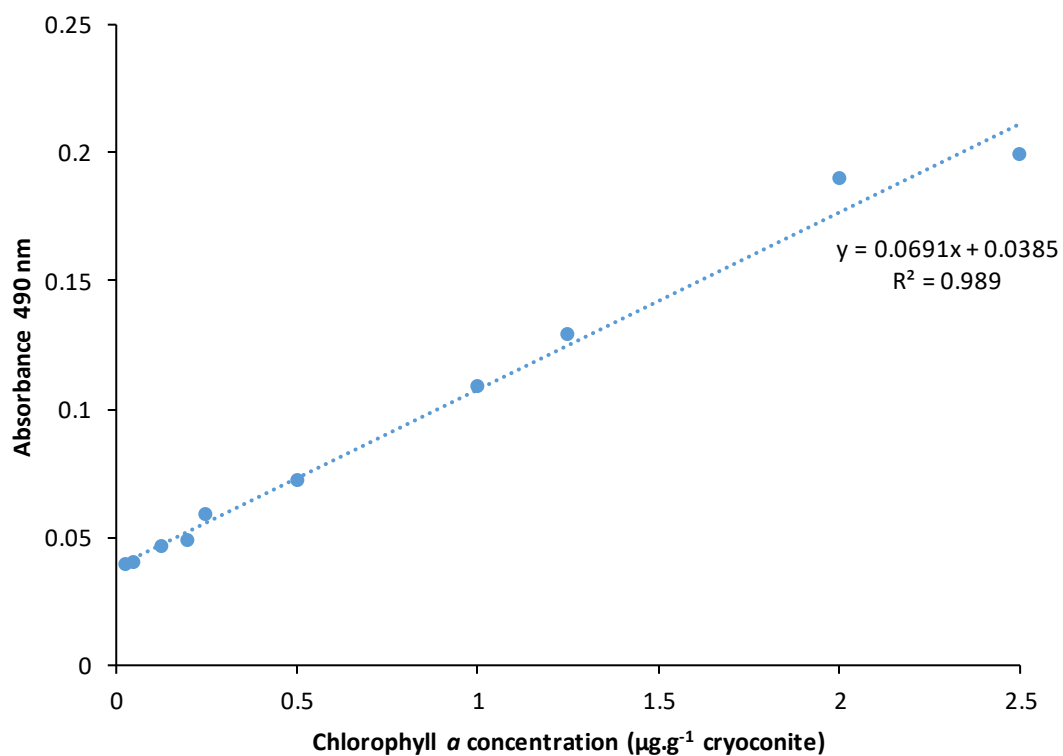


Figure IV. 1 Standard curve of chlorophyll *a*.

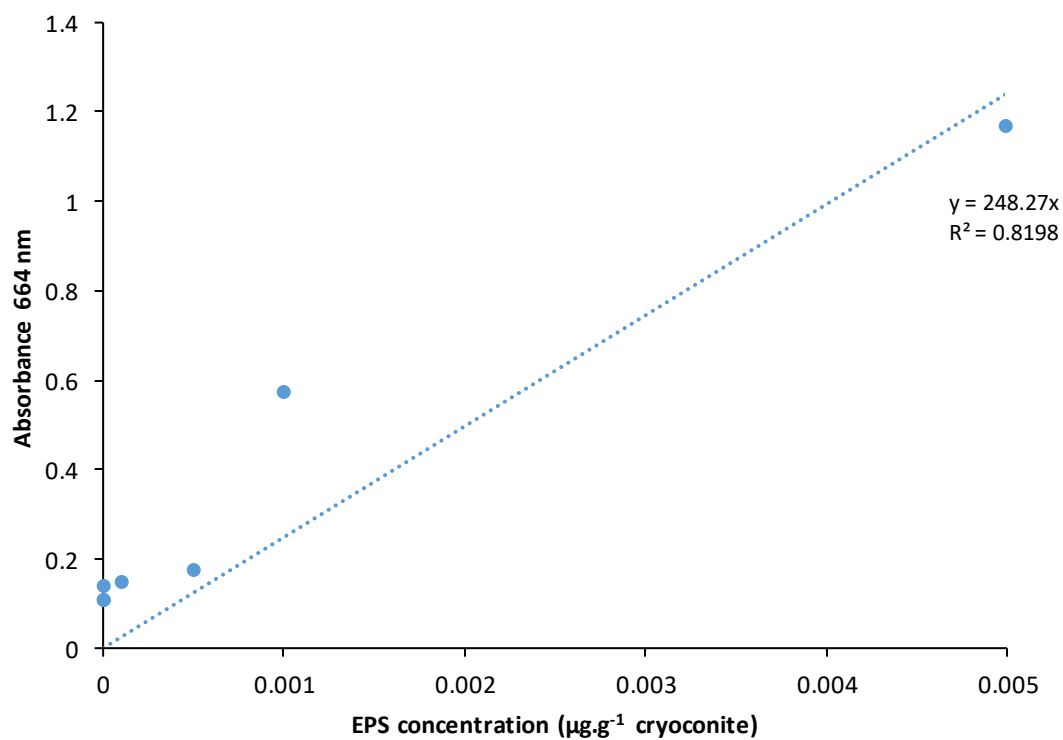


Figure IV. 2 Standard curve of mannose.

Table IV. 2 Sequential test of distLM model of environmental parameters on Foxfonna valley glacier.

Variable	Adj R2	SS(trace)	Pseudo-F	P	Proportion explained	Cumulative variance
EPS ($\mu\text{g.g}^{-1}$ cryoconite)	8.77E-02	25695	8.4973	0.001	9.94E-02	9.94E-02
Total IR (hrs)	0.11882	10865	3.72	0.001	4.20E-02	0.14141
E	0.13908	7958.9	2.7891	0.003	3.08E-02	0.1722
IR between sample collection (hrs)	0.14866	5201.8	1.8434	0.035	2.01E-02	0.19232
N	0.15623	4654.5	1.6643	0.074	1.80E-02	0.21032
Chl <i>a</i> ($\mu\text{g.g}^{-1}$ cryoconite)	0.16317	4452.4	1.6052	0.08	1.72E-02	0.22754
Curvature	0.16635	3521.3	1.2743	0.162	1.36E-02	0.24116
Elevation (Z, m)	0.16884	3342.4	1.2133	0.207	1.29E-02	0.25409
Slope (°)	0.16906	2805.4	1.0186	0.389	1.09E-02	0.26494

Table IV. 3 Marginal tests of distLM model of environmental parameters on Foxfonna valley glacier. Aspect is in degrees (0 = N, 90 = E).

Variable	SS(trace)	Pseudo-F	P	Proportion explained
EPS ($\mu\text{g.g}^{-1}$ cryoconite)	25695	8.4973	0.001	9.94E-02
Total IR (hrs)	21425	6.9577	0.001	8.29E-02
Chl <i>a</i> ($\mu\text{g.g}^{-1}$ cryoconite)	18527	5.944	0.001	7.17E-02
IR between sample collection (hrs)	8165.4	2.5112	0.011	3.16E-02
E	7687.2	2.3596	0.012	2.97E-02
Elevation (Z, m)	7673.4	2.3553	0.014	2.97E-02
N	7627.8	2.3409	0.014	2.95E-02
Aspect (°)	5870.1	1.7889	0.044	2.27E-02
Slope (°)	5951.4	1.8143	0.052	2.30E-02
Curvature	3986.7	1.206	0.236	1.54E-02
FAA Dinf contrib area (m^2)	3415.8	1.0309	0.353	1.32E-02
FAA D8 contrib area (m^2)	2281	0.68541	0.823	8.82E-03

Table IV. 4 Marginal tests of distLM model of environmental and high abundance bacterial taxa on the bacterial community on Foxfonna valley glacier. Aspect is in degrees (0 = N, 90 = E).

Variable	SS(trace)	Pseudo-F	P	Proportion explained
denovo-33968	50511	18.697	0.001	0.19537
denovo-62735	39754	13.991	0.001	0.15377
EPS ($\mu\text{g.g}^{-1}$ cryoconite)	25695	8.4973	0.001	9.94E-02
Cumulative IR to DAY (hrs)	21425	6.9577	0.001	8.29E-02
Chl <i>a</i> ($\mu\text{g.g}^{-1}$ cryoconite)	18527	5.944	0.001	7.17E-02
denovo-19355	16283	5.1756	0.001	6.30E-02
denovo-32859	15312	4.8476	0.001	5.92E-02
denovo-17849	10997	3.4207	0.002	4.25E-02
denovo-20155	9364.8	2.8939	0.002	3.62E-02
IR between sample collection (hrs)	8165.4	2.5112	0.004	3.16E-02
Elevation (Z, m)	7673.4	2.3553	0.012	2.97E-02
N	7627.8	2.3409	0.012	2.95E-02
E	7687.2	2.3596	0.017	2.97E-02
Slope (°)	5951.4	1.8143	0.049	2.30E-02
Aspect (°)	5870.1	1.7889	0.061	2.27E-02
denovo-57929	4623.7	1.4022	0.205	1.79E-02
Curvature	3986.7	1.206	0.221	1.54E-02
FAA Dinf (m^2)	3415.8	1.0309	0.369	1.32E-02
FAA D8 (m^2)	2281	0.68541	0.836	8.82E-03

Table IV. 5 Sequential tests of distLM model of environmental and high abundance bacterial taxa on the bacterial community on Foxfonna valley glacier.

Variable	Adj R ²	SS(trace)	Pseudo-F	P	Proportion explained	Cumulative variance
denovo-33968	0.18492	50511	18.697	0.001	0.19537	0.19537
denovo-62735	0.28762	28572	12.101	0.001	0.11052	0.30589
Elevation (Z, m)	0.30947	7791.3	3.404	0.001	3.01E-02	0.33603
denovo-17849	0.329	7080.4	3.1835	0.001	2.74E-02	0.36341
denovo-19355	0.34487	6063.1	2.7921	0.001	2.35E-02	0.38686
denovo-20155	0.35824	5363.3	2.5214	0.001	2.07E-02	0.40761
Chl <i>a</i> ($\mu\text{g.g}^{-1}$ cryoconite)	0.36798	4417.9	2.1089	0.003	1.71E-02	0.4247
E	0.38555	3996.7	1.9624	0.004	1.55E-02	0.45645
denovo-32859	0.3771	4212.8	2.0405	0.008	1.63E-02	0.44099
IR between sample collection (hrs)	0.40299	3253.3	1.644	0.016	1.26E-02	0.49484
Curvature	0.41155	2901.3	1.4875	0.039	1.12E-02	0.52472
Total IR (hrs)	0.39725	2789.6	1.3963	0.057	1.08E-02	0.48226
denovo-57929	0.39374	3882.2	1.9319	0.061	1.50E-02	0.47147
N	0.40707	2393.6	1.2179	0.155	9.26E-03	0.51349
Slope (°)	0.41339	2327.2	1.1969	0.187	9.00E-03	0.53372
EPS ($\mu\text{g.g}^{-1}$ cryoconite)	0.40508	2429.1	1.2319	0.229	9.40E-03	0.50424

Table IV. 6 Diversity statistics calculated for samples on Foxfonna valley glacier.

Sample	Number of OTUs (S)	Pielou's evenness (J')	Shannon Index (H'(Log _e))
202.FL2C2	19	0.988912	2.911792
202.FL2C5	24	0.969703	3.08177
202.FL4C1	20	0.985789	2.953159
202.FL4C3	1	-	0
202.FL4C4	13	0.97902	2.511135
202.FL4C5	15	0.947793	2.566672
202.FLC1A	10	0.985714	2.26969
202.FLC1B	6	0.877469	1.572213
202.FLC3A	29	0.988248	3.327724
202.FLC4A	32	0.984484	3.411962
202.FLC8A	21	0.958223	2.917333
210.FL2C1	16	0.919992	2.550759
210.FL2C1A	15	0.94356	2.555207
210.FL2C2	77	0.984405	4.276065
210.FL2C3	24	0.965218	3.067514
210.FL2C4	121	0.990952	4.752399
210.FL2C5	92	0.986393	4.460263
210.FL4C2	18	0.937948	2.711018
210.FLC1A	79	0.98365	4.298008
210.FLC2A	37	0.976508	3.52609
210.FLC3B	134	0.991068	4.85409
210.FLC4A	134	0.990982	4.853672
210.FLC4B	143	0.992212	4.924194
210.FLC5A	122	0.990172	4.756806
210.FLC5B	41	0.967728	3.593729
210.FLC8A	18	0.969889	2.803341
217.FL2C1	54	0.979548	3.9074
217.FL2C2	94	0.987865	4.488161
217.FL2C3	5	0.89191	1.435474
217.FL2C5	85	0.985602	4.378686
217.FL4C1	82	0.985149	4.341274
217.FL4C1A	142	0.990973	4.91109
217.FL4C4	99	0.98636	4.53244
217.FLC2A	98	0.987728	4.528701
217.FLC2B	38	0.974285	3.544046
217.FLC4B	107	0.988538	4.619268
217.FLC5A	150	0.991608	4.968584
217.FLC5B	136	0.989964	4.863349
217.FLC7A	75	0.984266	4.249555
217.FLC7B	67	0.982219	4.129928
217.FLC8B	81	0.985807	4.332077

Table IV. 6 Diversity statistics calculated for samples on Foxfonna valley glacier (continued).

Sample	Number of OTUs (S)	Pielou's evenness (J')	Shannon Index (H'(Log_e))
221.FL2C1	28	0.953429	3.177019
221.FL2C3	128	0.990017	4.803591
221.FL4C1	135	0.991327	4.862732
221.FL4C1A	74	0.98492	4.239161
221.FL4C3	25	0.956715	3.079545
221.FL4C4	15	0.928657	2.51485
221.FL4C5	92	0.986184	4.459317
221.FLC1A	71	0.980807	4.180868
221.FLC2A	62	0.981618	4.05127
221.FLC3A	107	0.987985	4.616686
221.FLC4A	123	0.990259	4.765309
221.FLC4B	136	0.991055	4.868713
221.FLC5A	121	0.990628	4.750844
221.FLC5B	42	0.975419	3.645794
221.FLC7A	116	0.989039	4.701485
221.FLC8A	49	0.980565	3.816181
221.FLC8B	153	0.991877	4.989574
228.FL2C1	24	0.952034	3.025615
228.FL2C2	38	0.969184	3.52549
228.FL2C3	39	0.969424	3.551544
228.FL2C4	93	0.988225	4.47923
228.FL2C5	22	0.956973	2.958045
228.FL4C1	32	0.969301	3.359341
228.FL4C2	39	0.968087	3.546646
228.FL4C3	37	0.972859	3.512916
228.FL4C4	38	0.970093	3.528798
228.FL4C5	31	0.962015	3.303547
228.FLC1A	23	0.954233	2.991993
228.FLC1B	104	0.986494	4.581665
228.FLC3A	25	0.949585	3.056597
228.FLC4A	37	0.966705	3.490693
228.FLC4B	121	0.98986	4.747164
228.FLC5A	20	0.943303	2.825883
228.FLC5B	34	0.964274	3.400378
228.FLC7A	77	0.98456	4.276738
228.FLC7B	133	0.991	4.846335
228.FLC8A	139	0.992183	4.895899
228.FLC8B	153	0.99141	4.987228

Table IV. 7 Marginal tests of distLM model predicting the effect of high abundance taxa and environmental variables on the total valley glacier bacterial community on DOY 202. Aspect is in degrees (0 = N, 90 = E).

Variable	SS(trace)	Pseudo-F	P	Proportion explained
denovo-16065	8657	2.8863	0.002	0.24283
denovo-5105	7778.8	2.5118	0.002	0.21819
denovo-12072	7736.4	2.4943	0.011	0.217
denovo-20567	6549.8	2.0256	0.012	0.18372
denovo-18137	4632.3	1.3441	0.02	0.12994
denovo-21394	7558.2	2.4214	0.021	0.21201
denovo-47295	7818.4	2.5282	0.022	0.2193
denovo-12431	5201.3	1.5373	0.031	0.14589
denovo-62144	4607.1	1.3356	0.081	0.12923
E	5061.1	1.489	0.099	0.14196
N	5012.2	1.4723	0.099	0.14059
Aspect (°)	4924.5	1.4424	0.099	0.13813
denovo-49069	4607.1	1.3356	0.099	0.12923
denovo-56073	3869.2	1.0957	0.111	0.10853
Elevation (Z, m)	4977.1	1.4603	0.117	0.13961
denovo-19355	4418.2	1.2731	0.149	0.12393
denovo-56948	3845.7	1.0882	0.175	0.10787
Slope (°)	4439.6	1.2802	0.186	0.12453
denovo-29496	4160.1	1.1889	0.209	0.11669
denovo-13946	3729.1	1.0514	0.266	0.1046
denovo-36688	3729.1	1.0514	0.281	0.1046
FAA Dinf (m ²)	4059.1	1.1564	0.289	0.11386
denovo-24255	3716	1.0473	0.352	0.10423
denovo-5852	3613.7	1.0152	0.435	0.10136
denovo-26477	3560.6	0.9986	0.522	0.099874
denovo-4244	3571.8	1.0021	0.536	0.10019
FAA D8 (m ²)	3346.3	0.93227	0.781	0.093862
denovo-30845	3424	0.95621	0.811	0.096042
Curvature	2644.7	0.72114	0.819	0.074182
denovo-4660	3198.5	0.88703	0.835	0.089717
denovo-5110	2443.8	0.66235	0.988	0.068549
Total IR (hrs)	0	0	1	0
IR between sample collection (hrs)	0	0	1	0
denovo-16065	8657	2.8863	0.002	0.24283
denovo-5105	7778.8	2.5118	0.002	0.21819

Table IV. 8 Sequential tests of distLM model predicting the effect of high abundance taxa and environmental parameters on valley glacier bacterial communities on DOY 202.

Variable	Adj R2	SS(trace)	Pseudo-F	P	Proportion explained	Cumulative variance
denovo-16065	0.1587	8657	2.8863	0.001	0.24283	0.24283
denovo-47295	0.28176	6509.2	2.5421	0.005	0.18258	0.42541
denovo-29496	0.44224	3949.9	1.9864	0.026	0.11079	0.66534
denovo-18137	0.36364	4604	2.0294	0.059	0.12914	0.55455
denovo-24255	0.98621	1438.8	29.264	0.096	0.040357	0.99862
denovo-12431	0.70222	2735.5	2.5768	0.159	0.07673	0.91067
E	0.51392	3266.2	1.8848	0.177	0.091616	0.75696
denovo-4660	0.58484	2744.3	1.8542	0.222	0.076978	0.83394
denovo-4244	0.79132	1696.9	2.2808	0.235	0.047597	0.95826
denovo-36688	0.98621	1.65E-11	0	1	4.63E-16	0.99862
-denovo-29496	0.98621	-1.4E-12	0	1	-3.9E-17	0.99862

Table IV. 9 Marginal tests of distLM model predicting the effect of high abundance taxa and environmental parameters on valley glacier bacterial communities on DOY 210. Aspect is in degrees (0 = N, 90 = E).

Variable	SS(trace)	Pseudo-F	P	Proportion explained
denovo-33968	8541.5	3.2985	0.002	0.20238
denovo-62735	5988.4	2.1496	0.015	0.14189
E	5780.3	2.063	0.02	0.13696
N	5192.4	1.8238	0.036	0.12303
Elevation (Z, m)	5330.2	1.8792	0.042	0.12629
denovo-8678	5637.2	2.0041	0.064	0.13357
denovo-12431	5637.2	2.0041	0.075	0.13357
Curvature	4800.2	1.6683	0.079	0.11374
Slope (°)	4623.3	1.5993	0.08	0.10954
denovo-53533	5020.4	1.7552	0.094	0.11895
FAA D8 (m ²)	4976.3	1.7377	0.108	0.11791
denovo-5379	4993	1.7443	0.117	0.11831
denovo-15498	5032.2	1.7599	0.14	0.11923
denovo-20155	4342.9	1.4912	0.188	0.1029
denovo-18395	4405.8	1.5153	0.274	0.10439
Aspect (°)	3435.5	1.152	0.289	0.081402
denovo-17849	3619.9	1.2196	0.298	0.08577
denovo-30379	3612	1.2167	0.33	0.085582
Total IR (hrs)	2802.4	0.92461	0.475	0.066401
IR between sample collection (hrs)	2802.4	0.92461	0.486	0.066401
FAA Dinf (m ²)	2735.3	0.90094	0.497	0.064811

Table IV. 10 Sequential tests of distLM model predicting the effect of high abundance taxa and environmental parameters on valley glacier bacterial communities on DOY 210.

Variable	Adj R2	SS(trace)	Pseudo-F	P	Proportion explained	Cumulative variance
denovo-33968	0.14103	8541.5	3.2985	0.001	0.20238	0.20238
denovo-62735	0.25827	4524.4	2.0234	0.023	0.1072	0.41721
denovo-12431	0.40001	3862.5	2.1355	0.026	0.091519	0.61429
denovo-20155	0.19501	4542.3	1.8718	0.065	0.10763	0.31001
denovo-30379	0.33188	4455.2	2.212	0.066	0.10556	0.52277
denovo-17849	0.4616	3294.2	2.0296	0.111	0.078052	0.69234
Slope (°)	0.57507	2601.4	2.0307	0.112	0.061637	0.81789
Total IR (hrs)	0.68602	1855.8	1.9606	0.127	0.043971	0.91029
denovo-18395	0.5125	2697.2	1.8353	0.141	0.063908	0.75625
Curvature	0.6257	2044.2	1.8116	0.228	0.048434	0.86632
FAA D8 (m ²)	0.72709	1317.9	1.6019	0.229	0.031226	0.94152
denovo-53533	0.773	1099.6	1.6068	0.309	0.026053	0.96757
FAA Dinf (m ²)	0.84547	902.76	1.9378	0.457	0.02139	0.98896
denovo-8678	0.84547	1.43E-11	0	1	3.39E-16	0.98896

Table IV. 11 Sequential tests of distLM model predicting the effect of high abundance taxa and environmental parameters on valley glacier bacterial communities on DOY 217. Aspect is in degrees (0 = N, 90 = E).

Variable	Adj R2	SS(trace)	Pseudo-F	P	Proportion explained	Cumulative variance
denovo-32859	0.30023	2797.7	1.8911	0.003	0.094523	0.45018
denovo-17849	0.24827	3550	2.2337	0.004	0.11994	0.35566
denovo-33714	0.17693	6976.9	4.0095	0.008	0.23572	0.23572
denovo-62735	0.34647	2456.9	1.7783	0.015	0.08301	0.53319
denovo-33968	0.3971	2345	1.8397	0.031	0.079226	0.61242
Aspect (°)	0.43026	1835.6	1.5239	0.099	0.062016	0.67443
denovo-33713	0.49226	1598.5	1.4891	0.165	0.054007	0.7824
denovo-20155	0.45678	1597	1.3905	0.179	0.053955	0.72839
FAA Dinf (m ²)	0.53132	1486.4	1.5001	0.223	0.050218	0.83261
N	0.60466	1179.4	1.411	0.31	0.039846	0.91528
Curvature	0.66058	1072.3	1.4943	0.315	0.036228	0.95151
denovo-15849	0.56403	1267.5	1.3752	0.319	0.042824	0.87544
Elevation (Z, m)	0.77126	951.58	1.9677	0.337	0.03215	0.98366

Table IV. 12 Marginal tests of distLM model predicting the effect of high abundance taxa and environmental parameters on valley glacier bacterial communities on DOY 217. Aspect is in degrees (0 = N, 90 = E).

Variable	SS(trace)	Pseudo-F	P	Proportion explained
denovo-62735	5001.9	2.6437	0.001	0.16899
Elevation (Z, m)	3777.4	1.9018	0.008	0.12762
denovo-33714	6976.9	4.0095	0.009	0.23572
E	3645.6	1.8261	0.011	0.12317
N	3619	1.811	0.012	0.12227
denovo-33968	4408.2	2.275	0.02	0.14894
IR between sample collection (hrs)	3706	1.8607	0.041	0.12521
denovo-17849	3269.5	1.6143	0.064	0.11046
denovo-32859	3428.6	1.7032	0.066	0.11584
Total IR (hrs)	3476.2	1.73	0.075	0.11745
denovo-33713	6949.1	3.9886	0.077	0.23478
denovo-15849	3098.8	1.5202	0.089	0.10469
denovo-18364	3195.3	1.5733	0.112	0.10796
denovo-38076	2524.3	1.2121	0.152	0.085286
denovo-20155	2668.1	1.288	0.155	0.090145
denovo-13192	2488.8	1.1935	0.232	0.084087
Aspect (°)	2039.4	0.96202	0.451	0.068902
FAA Dinf (m ²)	1912.2	0.8979	0.55	0.064607
Curvature	1893.8	0.88866	0.55	0.063985
Slope (°)	1741	0.81248	0.709	0.058822
FAA D8 (m ²)	1245.7	0.57119	0.934	0.042089

Table IV. 13 Marginal tests of distLM model predicting the effect of high abundance taxa and environmental parameters on valley glacier bacterial communities on DOY 221. Aspect is in degrees (0 = N, 90 = E).

Variable	SS(trace)	Pseudo-F	P	Proportion explained
denovo-33968	6348.3	3.1546	0.003	0.17376
denovo-62735	5419.5	2.6127	0.02	0.14834
denovo-32859	4225.3	1.9617	0.028	0.11565
N	3954	1.8204	0.045	0.10823
denovo-17849	4187.5	1.9419	0.048	0.11462
E	3910.4	1.7979	0.051	0.10703
Elevation (Z, m)	3941.4	1.8139	0.057	0.10788
Aspect (°)	3616.4	1.6479	0.062	0.098987
denovo-57929	5775.8	2.8167	0.064	0.15809
denovo-38076	3635.9	1.6578	0.083	0.099521
IR between sample collection (hrs)	3427.1	1.5527	0.086	0.093804
denovo-5379	3722.2	1.7016	0.133	0.10188
Slope (°)	3125.3	1.4032	0.137	0.085543
denovo-53742	2997.9	1.3409	0.151	0.082056
denovo-20155	2922.7	1.3043	0.183	0.079999
Total IR (hrs)	2832.1	1.2605	0.189	0.077519
denovo-57985	2817.2	1.2533	0.227	0.07711
FAA Dinf (m ²)	2273.5	0.9954	0.323	0.06223
Curvature	1739.1	0.74973	0.733	0.047603
FAA D8 (m ²)	1610.2	0.69157	0.804	0.044073

Table IV. 14 Sequential tests of distLM model predicting the effect of high abundance taxa and environmental parameters on valley glacier bacterial communities on DOY 221. Aspect is in degrees (0 = N, 90 = E).

Variable	Adj R2	SS(trace)	Pseudo-F	P	Proportion explained	Cumulative variance
denovo-33968	0.11868	6348.3	3.1546	0.001	0.17376	0.17376
IR between sample collection (hrs)	0.2995	3414.5	2.1347	0.006	0.093459	0.47463
denovo-32859	0.1922	4362.6	2.3651	0.01	0.11941	0.29317
denovo-38076	0.23836	3214.8	1.8485	0.028	0.087994	0.38117
denovo-62735	0.34101	2642.2	1.7559	0.039	0.072321	0.54695
denovo-57929	0.37777	2344	1.6497	0.059	0.064158	0.6111
denovo-57985	0.4194	2276.4	1.7171	0.081	0.062308	0.67341
denovo-20155	0.45727	2017.6	1.6281	0.092	0.055225	0.72864
denovo-5379	0.4867	1709.5	1.4586	0.171	0.046793	0.77543
Aspect (°)	0.50697	1493.6	1.3267	0.264	0.040881	0.7843
FAA D8 (m ²)	0.6315	1236.4	1.4694	0.318	0.033842	0.95394
denovo-53742	0.52438	1364.2	1.2561	0.323	0.03734	0.82164
Total IR (hrs)	0.54171	1283.9	1.2269	0.332	0.035143	0.85678
denovo-17849	0.57384	1121.6	1.1526	0.343	0.030699	0.9201
Curvature	0.55758	1191.4	1.1794	0.367	0.032612	0.8894
IR between sample collection (hrs)	0.66363	914.8	1.1911	0.435	0.025039	0.97898
-IR between sample collection (hrs)	0.48684	1169.5	0.99779	0.463	0.032011	0.74342

Table IV. 15 Marginal tests of distLM model predicting the effect of high abundance taxa and environmental parameters on valley glacier bacterial communities on DOY 228. Aspect is in degrees (0 = N, 90 = E).

Variable	SS(trace)	Pseudo-F	P	Proportion explained
denovo-62735	22735	13	0.001	0.40625
denovo-33968	21467	11.824	0.001	0.38359
denovo-57985	3901.7	1.424	0.094	0.06972
N	3885.4	1.4176	0.165	0.069428
Elevation (Z, m)	3765.1	1.3705	0.177	0.06728
E	3764.4	1.3703	0.184	0.067267
Slope (°)	3490.4	1.2639	0.214	0.062372
Aspect (°)	3545.1	1.285	0.227	0.063349
FAA Dinf (m ²)	3317	1.1971	0.258	0.059272
Curvature	3265.1	1.1772	0.263	0.058345
FAA D8 (m ²)	3054.3	1.0968	0.309	0.054578
Total IR (hrs)	2403.3	0.85258	0.447	0.042946
IR between sample collection (hrs)	2473	0.87843	0.472	0.04419

Table IV. 16 Sequential tests of distLM model predicting the effect of high abundance taxa and environmental parameters on valley glacier bacterial communities on DOY 228.

Variable	Adj R2	SS(trace)	Pseudo-F	P	Proportion explained	Cumulative variance
denovo-62735	0.375	22735	13	0.001	0.40625	0.40625
N	0.41869	3949	2.4278	0.001	0.070566	0.47682
E	0.43606	2453	1.5546	0.032	0.043834	0.52065
denovo-33968	0.4683	2228.5	1.4979	0.075	0.039822	0.60122
denovo-57985	0.45175	2280.4	1.4866	0.091	0.04075	0.5614
Slope (°)	0.50709	2075.2	1.5046	0.111	0.037082	0.70425
Total IR (hrs)	0.48796	1857.6	1.2965	0.189	0.033194	0.66717
Curvature	0.47711	1833	1.2529	0.207	0.032755	0.63398
Elevation (Z, m)	0.51209	1533.2	1.123	0.325	0.027397	0.73165
IR between sample collection (hrs)	0.51387	1414.9	1.0402	0.426	0.025284	0.75694

Table IV. 17 Marginal tests of distLM model of environmental variables, core taxa and keystone taxa on metabolites from Foxfonna glacier cryconite. Aspect is in degrees (0 = N, 90 = E).

Variable	SS(trace)	Pseudo-F	P	Proportion explained
denovo-33968	560.56	1.8831	0.013	2.3872E-2
denovo-62735	377.49	1.258	0.179	1.6075E-2
denovo-19355	322.56	1.0724	0.141	1.3736E-2
denovo-20155	192.47	0.63635	0.908	8.1965E-3
denovo-17849	225.4	0.74625	0.72	9.5985E-3
denovo-32859	337.34	1.1223	0.167	1.4365E-2
denovo-57929	212.86	0.70435	0.53	9.0645E-3
N	214.76	0.7107	0.938	9.1454E-3
E	255.09	0.84565	0.696	1.0863E-2
Elevation (Z, m)	228.62	0.75702	0.859	9.7357E-3
Slope (°)	206.06	0.68167	0.953	8.7752E-3
Aspect (°)	250.55	0.83041	0.668	1.067E-2
Curvature	437.45	1.4616	0.098	1.8629E-2
FAA D8 (m ²)	255.98	0.84863	0.382	1.0901E-2
FAA Dinf (m ²)	400.82	1.3371	0.139	1.7069E-2
Total IR (hrs)	430.52	1.4381	0.076	1.8334E-2
IR between sample collection (hrs)	342.82	1.1408	0.185	1.4599E-2
Chl <i>a</i> (µg.g ⁻¹ cryoconite)	1188.6	4.1054	0.015	5.0618E-2
EPS (µg.g ⁻¹ cryoconite)	535	1.7952	0.048	2.2783E-2

Table IV. 18 Sequential tests of distLM model of environmental variables, core taxa and keystone taxa on metabolites from Foxfonna valley glacier cryoconite.

Variable	Adj R ²	SS(trace)	Pseudo-F	P	Proportion explained	Cumulative variance
Chl <i>a</i> (µg.g ⁻¹ cryoconite)	3.8289E-2	1188.6	4.1054	0.01	5.0618E-2	5.0618E-2
IR between sample collection (hrs)	4.1791E-2	369.66	1.2814	0.106	1.5742E-2	6.636E-2
denovo-33968	4.4693E-2	354	1.2309	0.131	1.5075E-2	8.1435E-2
Curvature	4.6676E-2	331.79	1.156	0.2	1.4129E-2	9.5564E-2
denovo-32859	4.6738E-2	288.36	1.0048	0.275	1.228E-2	0.10784

Table IV. 19 Tentative metabolite ID of importance classified by day and site ($P < 0.01$, FDR < 0.01) established by post hoc ANOVA filtering using Metaboanalyst 3.0

Tentative Metabolite ID	F value	P value	False Discovery Rate
3',5'-cyclic IMP	14.749	1.06E-18	1.67E-15
Pantetheine-4'-phosphate	11.968	6.73E-16	4.56E-13
Hydroxylamine	11.864	8.69E-16	4.56E-13
Chloramines	11.366	3.03E-15	1.19E-12
Phosphinate	10.138	7.47E-14	2.35E-11
Uracil	8.5294	6.74E-12	1.77E-09
Hydroxypyruvic acid	7.3989	2.00E-10	4.49E-08
Hypoxanthine	7.102	5.03E-10	9.90E-08
Caprylic acid	7.0553	5.83E-10	1.02E-07
m/z 77.81	6.3944	4.82E-09	6.89E-07
m/z 41.9	6.1332	1.13E-08	1.49E-06
Chloroacetaldehyde	5.8778	2.64E-08	3.20E-06
m/z 45.9	5.7825	3.63E-08	4.02E-06
Phosphoramidate	5.7664	3.84E-08	4.02E-06
2-Oxobutanoate	5.6286	6.10E-08	5.99E-06
Ergosta-5,7,22,24(28)-tetraen-3-b-ol	5.5714	7.40E-08	6.81E-06
Malic acid	5.5563	7.79E-08	6.81E-06
Urea	5.5183	8.86E-08	7.33E-06
m/z 64.9	5.0655	4.19E-07	3.17E-05
dAMP	5.063	4.23E-07	3.17E-05
3-hydroxyanthranilate	5.0033	5.20E-07	3.72E-05
Hydrogen sulfite	4.9636	5.97E-07	4.08E-05
Cystine	4.691	1.55E-06	9.38E-05
Tetracosatetraenoic acid (24:4n-6)	4.6378	1.87E-06	0.000109
m/z 57.9	4.5496	2.56E-06	0.000139
Ethylene glycol	4.5493	2.56E-06	0.000139
Glyceric acid	4.5164	2.87E-06	0.000151
Indole-3-pyruvate	4.3654	4.92E-06	0.000238
Shikimate-3-phosphate	4.3611	4.99E-06	0.000238
3-Aminopropane-1,2-diol	4.2384	7.75E-06	0.000358
Spermidine	4.2213	8.24E-06	0.00037
Proline	4.1417	1.10E-05	0.000475
Glyceric acid	4.1365	1.12E-05	0.000475
Ethanolamine	4.104	1.26E-05	0.000507
Maltose	4.1034	1.26E-05	0.000507
3-Aminopropanal	4.0507	1.52E-05	0.000586
Oxalic acid	4.0496	1.53E-05	0.000586
Guanine	4.037	1.60E-05	0.000599
Thymidine	4.0009	1.82E-05	0.000636
2-Methylmalic acid	3.9874	1.91E-05	0.000654
Benzoic acid	3.9396	2.27E-05	0.000729
m/z 26	3.9287	2.36E-05	0.000743

Table IV. 19 Tentative metabolite ID of importance classified by day and site ($P < 0.01$, FDR < 0.01) established by post hoc ANOVA filtering using Metaboanalyst 3.0 (continued).

Tentative Metabolite ID	F value	P value	False Discovery Rate
S-formylglutathione	3.9175	2.46E-05	0.000759
Sedoheptulose-1,7-bisphosphate	3.9095	2.53E-05	0.000766
Citric acid	3.8713	2.91E-05	0.000863
(1'S)-Averantin	3.8643	2.98E-05	0.000869
Glycolic acid	3.8516	3.12E-05	0.000879
Salicylic acid	3.8462	3.19E-05	0.000879
Glycerol	3.8377	3.29E-05	0.000891
Pantothenic acid	3.7933	3.86E-05	0.001012
1-(5'-phosphoribosyl)-5-formamido-4-imidazolecarboxamide	3.7509	4.50E-05	0.001107
Mannose-6-phosphate	3.7173	5.09E-05	0.001231
Glucono-1,5-lactone-6-phosphate	3.7077	5.27E-05	0.001255
Protoviolaceinic acid	3.6945	5.53E-05	0.001297
Fumaric acid	3.6224	7.19E-05	0.001615
Glycine	3.5789	8.42E-05	0.001839
(RS)-phospho-3-sulfolactate	3.5526	9.27E-05	0.001997
Asparaginy-Phenylalanine	3.5283	0.000101	0.002096
Acetyl phosphate	3.4766	0.000122	0.002466
Deoxy-ribose-1-phosphate	3.4713	0.000125	0.002482
p-Benzoquinone	3.4394	0.00014	0.002692
Glutamate-5-semialdehyde	3.4374	0.000141	0.002692
Oxalosuccinate	3.4119	0.000155	0.0029
Oxalacetic acid	3.3777	0.000176	0.00321
Ribulose-1,5-bisphosphate	3.32	0.000217	0.003875
Spermine	3.3157	0.00022	0.003879
Nitrite	3.3135	0.000222	0.003879
2-oxoglutarate	3.2948	0.000238	0.003962
Ribonic acid	3.2519	0.000278	0.004374
Fructuronate	3.2449	0.000285	0.004398
Magnesium chloride	3.2206	0.000312	0.004716
Nitrosobenzene	3.1503	0.000403	0.005749
Chloroethane	3.1481	0.000406	0.005749
Geranyl phosphate	3.1411	0.000417	0.005802
Aminoimidazole ribotide	3.1331	0.000429	0.005923
7,8-diaminononanoate	3.1261	0.00044	0.006023
Naringenin	3.1211	0.000449	0.006082
4-(L-gamma-Glutamylamino)butanoate	3.1104	0.000466	0.006267
Hydroxycitrulline	3.0897	0.000503	0.006381
m/z 372.27	3.0867	0.000509	0.006381
Alanine	3.0863	0.000509	0.006381
(S)-Autumnaline	3.0832	0.000515	0.006381

Table IV. 19 Tentative metabolite ID of importance classified by day and site ($P < 0.01$, FDR < 0.01) established by post hoc ANOVA filtering using Metaboanalyst 3.0 (continued).

Tentative Metabolite ID	F value	P value	False Discovery Rate
Orotidylic acid	3.0776	0.000526	0.006461
Pelargonidin	3.074	0.000533	0.006496
Myristic acid	3.0621	0.000557	0.006651
N-acetylmuramic acid	3.0613	0.000558	0.006651
Formic acid	3.0374	0.000609	0.007096
Palmitic acid	3.0197	0.00065	0.00746
Isocitric acid	2.9731	0.00077	0.008533
Stearic acid	2.971	0.000776	0.00854
Dihydrokaempferol	2.9444	0.000855	0.00897
Glutathione	2.9358	0.000883	0.00909
Glyceric acid	2.9238	0.000922	0.00942
Glutamic acid	2.9195	0.000937	0.009421
Orotidine-5'-phosphate	2.9153	0.000951	0.009421
4-Phospho-L-aspartate	2.914	0.000956	0.009421
PRPP	2.9133	0.000958	0.009421
5-HPETE	2.9052	0.000987	0.009523

APPENDIX V

Supplementary Tables and Figures for “Chapter 7 - Seasonal dynamics and activity of supraglacial bacterial communities on the Greenland Ice Sheet”.

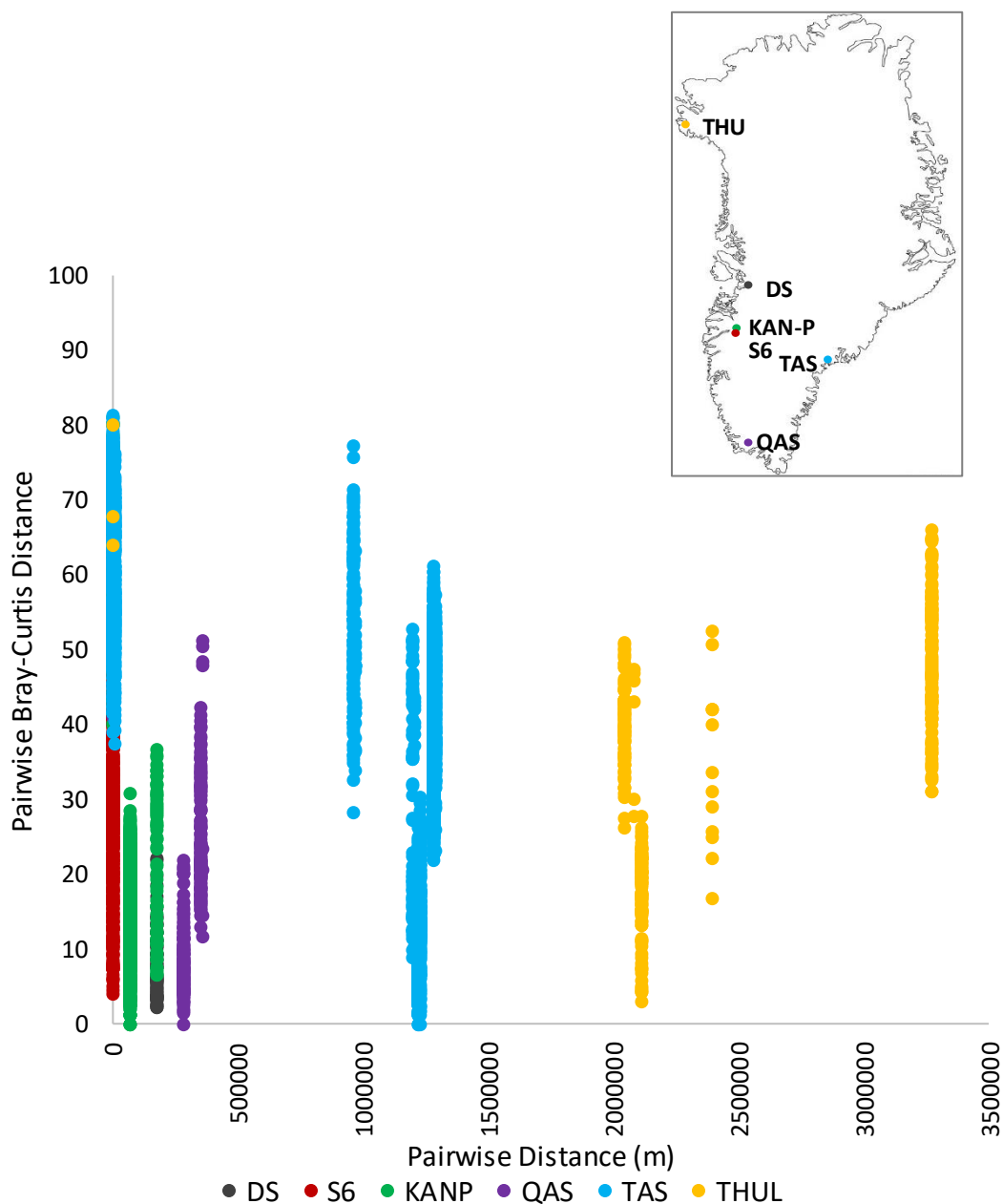


Figure V. 1 Pairwise Bray-Curtis distances and pairwise physical distance for sites on Greenland Ice Sheet Illulissat (DS), S6, Kangerlussuaq (KAN-P), Qaqortoq (QAS), Tasiilaq (TAS) and Thule (THU).

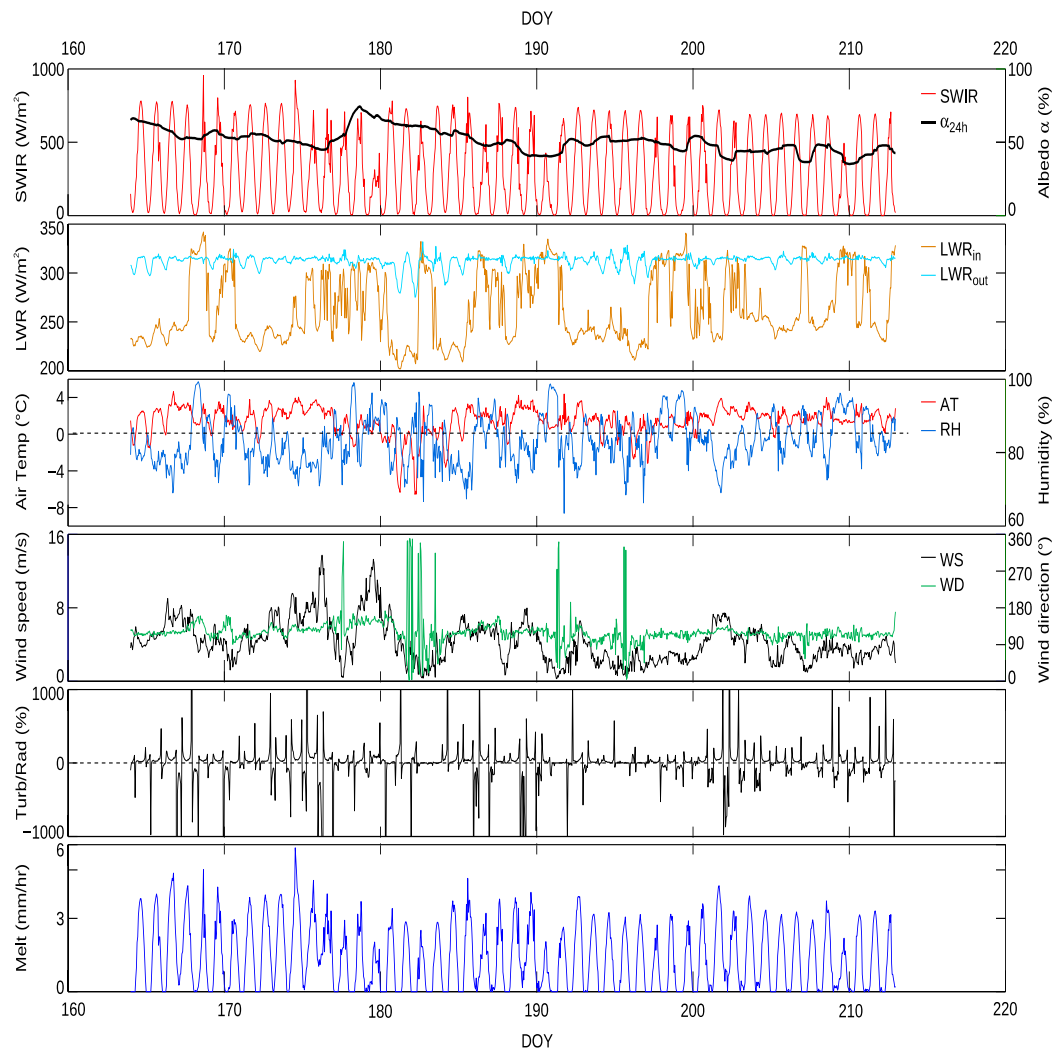


Figure V. 2 Meteorological data recorded by the S6 automated weather station showing conditions over the duration of the sampling season in 2014. Image credit: Dr. Tristram Irvine-Fynn.

Table V. 1 Diversity statistics recorded on GrIS S6.

Sample	Number of OTUs (S)	Pielou's Evenness (J')	Shannon Index (H'(log _e))
GrIScDNAcryo1.1	54	0.979401	3.906813
GrIScDNAcryo1.2	64	0.981003	4.079875
GrIScDNAcryo2.1	58	0.984101	3.995884
GrIScDNAcryo2.2	63	0.983086	4.07306
GrIScDNAcryo2.3	61	0.981413	4.034467
GrIScDNAcryo3.1	63	0.981203	4.065256
GrIScDNAcryo3.2	52	0.981156	3.876786
GrIScDNAcryo3.3	58	0.980234	3.980186
GrIScDNAcryo4.1	53	0.982874	3.902298
GrIScDNAcryo4.2	60	0.982314	4.021931
GrIScDNAcryo4.3	56	0.980899	3.948464
GrIScDNAcryo5.1	67	0.985117	4.142115
GrIScDNAcryo5.3	58	0.978768	3.974233
GrIScDNAcryo6.1	56	0.981739	3.951846
GrIScDNAcryo6.2	58	0.978802	3.97437
GrIScDNAcryo6.3	62	0.983305	4.058233
GrIScDNAsnow1.1	34	0.975048	3.43837
GrIScDNAsnow1.2	26	0.960267	3.128644
GrIScDNAsnow2.2	41	0.968486	3.596543
GrIScDNAsnow2.3	26	0.966828	3.150019
GrIScDNAsnow3.1	21	0.970255	2.953964
GrIScDNAsnow3.2	21	0.95997	2.922651
GrIScDNAsnow3.3	31	0.979424	3.363331
GrIScDNAsnow4.1	25	0.966047	3.109587
GrIScDNAsnow4.2	43	0.978071	3.678722
GrIScDNAsnow4.3	22	0.959713	2.966514
GrIScDNAsnow6.1	75	0.983606	4.246708
GrIScDNAsnow6.2	64	0.982186	4.084798
GrIScDNAsnow6.3	53	0.9797	3.889694
GrIScDNAsnow7.1	52	0.979988	3.872171
GrIScDNAsnow7.2	61	0.981707	4.035672
GrIScDNAsnow7.3	64	0.983799	4.091504
GrIScDNAstream1.3	40	0.976709	3.60296
GrIScDNAstream2.1	102	0.988849	4.5734
GrIScDNAstream2.2	111	0.989123	4.658303
GrIScDNAstream2.3	95	0.986759	4.493578
GrIScDNAstream3.1	78	0.985014	4.29142
GrIScDNAstream3.2	70	0.985194	4.185592
GrIScDNAstream4.2	95	0.987287	4.495982
GrIScDNAstream4.3	75	0.984043	4.248593
GrIScDNAstream5.1	46	0.977634	3.743011
GrIScDNAstream5.2	78	0.985186	4.292169
GrIScDNAstream5.3	86	0.984593	4.385717

Table V. 1 Diversity statistics recorded on GrIS S6 (continued).

Sample	Number of OTUs (S)	Pielou's Evenness (J')	Shannon Index (H'(log_e))
GrIScDNAstream6.1	101	0.987563	4.55772
GrIScDNAstream7.1	98	0.989005	4.534558
GrIScDNAstream7.2	94	0.988438	4.490764
GrIScDNAstream7.3	98	0.988163	4.530693
GrIScryo1.1	61	0.985166	4.049895
GrIScryo1.2	86	0.990012	4.409857
GrIScryo1.3	40	0.986624	3.639537
GrIScryo2.1	40	0.984094	3.630203
GrIScryo2.2	80	0.987975	4.329334
GrIScryo2.3	57	0.985318	3.98369
GrIScryo3.1	78	0.987364	4.301657
GrIScryo3.2	62	0.984697	4.063978
GrIScryo3.3	44	0.984959	3.727271
GrIScryo4.1	27	0.974922	3.213184
GrIScryo4.2	55	0.984597	3.945608
GrIScryo4.3	75	0.988109	4.266147
GrIScryo5.1	113	0.990339	4.681714
GrIScryo5.2	69	0.988152	4.183939
GrIScryo6.1	32	0.986696	3.419629
GrIScryo6.2	81	0.989338	4.347596
GrIScryo6.3	47	0.985562	3.794559
GrIScryo7.1	80	0.987358	4.326631
GrIScryo7.2	36	0.977775	3.503874
GrIScryo7.3	94	0.988997	4.493306
GrISsnow1.1	36	0.973496	3.488541
GrISsnow1.2	35	0.974897	3.466098
GrISsnow2.1	27	0.966508	3.185451
GrISsnow2.2	38	0.972446	3.537357
GrISsnow2.3	23	0.95478	2.993708
GrISsnow3.1	21	0.961843	2.928352
GrISsnow3.2	27	0.963066	3.17411
GrISsnow3.3	13	0.982447	2.519926
GrISsnow4.1	45	0.978559	3.725045
GrISsnow4.2	36	0.970292	3.477061
GrISsnow4.3	35	0.96862	3.44378
GrISsnow5.1	41	0.969535	3.600438
GrISsnow5.2	39	0.979299	3.587722
GrISsnow5.3	46	0.977	3.740584
GrISsnow6.1	45	0.975683	3.714095
GrISsnow6.2	42	0.976982	3.651634
GrISsnow6.3	52	0.978828	3.867587
GrISsnow7.1	53	0.976835	3.878319
GrISsnow7.2	42	0.974253	3.641435
GrISsnow7.3	51	0.979348	3.850624

Table V. 1 Diversity statistics recorded on GrIS S6 (continued).

Sample	Number of OTUs (S)	Pielou's Evenness (J')	Shannon Index (H'(log_e))
GrISstream1.2	31	0.971847	3.337309
GrISstream1.3	37	0.97783	3.530864
GrISstream2.1	126	0.990616	4.790897
GrISstream2.2	115	0.990086	4.697891
GrISstream2.3	123	0.990042	4.764263
GrISstream3.2	113	0.989111	4.675914
GrISstream3.3	113	0.989409	4.677322
GrISstream4.1	113	0.988373	4.672424
GrISstream4.2	104	0.987539	4.586518
GrISstream4.3	111	0.988957	4.657523
GrISstream5.1	121	0.989302	4.744486
GrISstream5.2	132	0.990012	4.834031
GrISstream5.3	128	0.990275	4.804844
GrISstream6.1	126	0.990325	4.789491
GrISstream6.2	129	0.990041	4.811415
GrISstream6.3	127	0.991377	4.802417
GrISstream7.1	128	0.990757	4.807183
GrISstream7.2	122	0.990075	4.756342
GrISstream7.3	122	0.990348	4.757652

Table V. 2 Marginal tests of distLM model predicting the effect of environmental conditions on 16S rRNA gene and 16S cDNA sequences on Greenland Ice Sheet surface habitats.

Variable	SS(trace)	Pseudo-F	P	Proportion explained
E	18344	5.7844	0.001	5.27E-02
N	14364	4.4755	0.001	4.13E-02
Day of year	14480	4.5132	0.001	4.16E-02
Total incoming SWR	14334	4.4657	0.001	4.12E-02
Average outgoing SWR	13065	4.0548	0.001	3.75E-02
SD outgoing SWR	14551	4.5363	0.001	4.18E-02
Total outgoing SWR	13846	4.3073	0.001	3.98E-02
Average albedo	12400	3.841	0.001	3.56E-02
Total incoming LWR	13668	4.2497	0.001	3.93E-02
Total Melt	14550	4.5359	0.001	4.18E-02
Total outgoing LWR	12094	3.7428	0.002	3.47E-02
Average incoming SWR	8390.4	2.5682	0.005	2.41E-02
SD outgoing LWR	7771.1	2.3743	0.012	2.23E-02
Average outgoing LWR	6170.8	1.8766	0.048	1.77E-02
SD incoming LWR	5525.5	1.6772	0.078	1.59E-02
SD Melt	4783.1	1.4487	0.138	1.37E-02
SD incoming SWR	3975.2	1.2012	0.255	1.14E-02
Total weekly PDD	3924.7	1.1857	0.264	1.13E-02
Average melt	3708.8	1.1198	0.319	1.07E-02
Total weekly PDH	3580.4	1.0806	0.346	1.03E-02
Average incoming LWR	3176.7	0.95768	0.477	9.12E-03
SD albedo	3012.9	0.90785	0.497	8.65E-03

Table V. 3 Sequential tests of distLM model predicting the effect of environmental parameters on 16S rRNA gene and 16S cDNA on Greenland Ice Sheet surfaces.

Variable	Adj R ²	SS(trace)	Pseudo-F	P	Proportion explained	Cumulative variance
N	0.20737	30248	11.18	0.001	8.69E-02	0.20737
Total outgoing SWR	0.12049	23606	7.9405	0.001	6.78E-02	0.12049
E	5.27E-02	18344	5.7844	0.001	5.27E-02	5.27E-02
Total Melt	0.22807	7205	2.7077	0.002	2.07E-02	0.22807
Day of year	0.23724	3193.3	1.2025	0.239	9.17E-03	0.23724
Total incoming LWR	0.24523	2780.7	1.0476	0.37	7.99E-03	0.24523
SD incoming SWR	0.25112	2051.4	0.77104	0.726	5.89E-03	0.25112
Average albedo	0.25517	1411.6	0.52801	0.962	4.05E-03	0.25517
SD incoming LWR	0.25517	-2.05E-11	0	1	-5.89E-17	0.25517

Table V. 4 Marginal tests of distLM model predicting the effect of environmental parameters on 16S rRNA gene and 16S cDNA cryoconite on Greenland Ice Sheet.

Variable	SS(trace)	Pseudo-F	P	Proportion explained
Average incoming LWR	2394.2	1.0369	0.325	2.96E-02
Average incoming SWR	2384.3	1.0325	0.344	2.95E-02
Average outgoing SWR	2136.3	0.92218	0.428	2.64E-02
SD outgoing LWR	2040.3	0.87965	0.485	2.52E-02
Average albedo	1943	0.8367	0.532	2.40E-02
Day of year	1903.6	0.81932	0.562	2.35E-02
E	1876.8	0.8075	0.571	2.32E-02
N	1876.8	0.8075	0.573	2.32E-02
SD outgoing SWR	1877.8	0.80793	0.575	2.32E-02
Average outgoing LWR	1906	0.82035	0.577	2.36E-02
Total weekly PDD	1819.5	0.78229	0.602	2.25E-02
Total incoming LWR	1820.1	0.78253	0.611	2.25E-02
Total weekly PDH	1813.5	0.77964	0.62	2.24E-02
Total outgoing LWR	1796	0.77194	0.626	2.22E-02
Total outgoing SWR	1776.7	0.76347	0.637	2.20E-02
SD albedo	1771.3	0.76111	0.638	2.19E-02
Total Melt	1770.4	0.76071	0.641	2.19E-02
Total incoming SWR	1786.5	0.76777	0.647	2.21E-02
SD incoming SWR	1756.8	0.75474	0.65	2.17E-02
Average melt	1777.7	0.76389	0.653	2.20E-02
SD incoming LWR	1640.3	0.70365	0.715	2.03E-02
SD Melt	1689.4	0.72514	0.72	2.09E-02

Table V. 5 Sequential tests of distLM model predicting the effect of environmental parameters on 16S rRNA gene and 16S cDNA cryoconite on Greenland Ice Sheet.

Variable	Adj R ²	SS(trace)	Pseudo-F	P	Proportion explained	Cumulative variance
Average incoming LWR	2.96E-02	2394.2	1.0369	0.307	2.96E-02	2.96E-02
Average incoming SWR	7.85E-02	2138	0.91772	0.439	2.64E-02	7.85E-02
SD incoming SWR	0.10285	1970.9	0.84182	0.51	2.44E-02	0.10285
E	5.21E-02	1817.1	0.78193	0.58	2.25E-02	5.21E-02
Total incoming LWR	0.12385	1699.2	0.71918	0.706	2.10E-02	0.12385
Total outgoing LWR	0.13592	976.76	0.40521	0.972	1.21E-02	0.13592

Table V. 6 Marginal tests of distLM model predicting the effect of environmental parameters on 16S rRNA gene and 16S cDNA snow on Greenland Ice Sheet.

Variable	SS(trace)	Pseudo-F	P	Proportion explained
Day of year	22339	8.4326	0.001	0.19873
Total incoming SWR	20520	7.5929	0.001	0.18255
Average outgoing SWR	19896	7.3121	0.001	0.177
SD outgoing SWR	20921	7.7752	0.001	0.18612
Total outgoing SWR	19585	7.174	0.001	0.17424
Average albedo	18472	6.686	0.001	0.16433
Total incoming LWR	20060	7.3857	0.001	0.17846
SD outgoing LWR	13833	4.7711	0.001	0.12306
Total outgoing LWR	17419	6.235	0.001	0.15497
Total Melt	20649	7.6513	0.001	0.1837
Average incoming SWR	12768	4.3567	0.003	0.11358
Average outgoing LWR	11022	3.6964	0.004	9.81E-02
E	8760.3	2.8737	0.009	7.79E-02
N	8760.3	2.8737	0.017	7.79E-02
Total weekly PDD	7296.2	2.3601	0.02	6.49E-02
SD incoming LWR	7115.7	2.2977	0.035	6.33E-02
Total weekly PDH	6714.2	2.1599	0.039	5.97E-02
Average melt	5672.5	1.807	0.06	5.05E-02
SD albedo	5610.5	1.7862	0.07	4.99E-02
Average incoming LWR	5707.2	1.8186	0.076	5.08E-02
SD Melt	5233.5	1.6603	0.119	4.66E-02
SD incoming SWR	2883.8	0.89524	0.483	2.57E-02

Table V. 7 Sequential tests of distLM model predicting the effect of environmental parameters on 16S rRNA gene and 16S cDNA snow on Greenland Ice Sheet.

Variable	Adj R ²	SS(trace)	Pseudo-F	P	Proportion explained	Cumulative variance
Day of year	0.19873	22339	8.4326	0.001	0.19873	0.19873
SD outgoing SWR	0.25136	5916.3	2.3201	0.021	5.26E-02	0.25136
SD albedo	0.2939	4781.5	1.9277	0.058	4.25E-02	0.2939
Average outgoing LWR	0.33374	4478	1.8536	0.063	3.98E-02	0.33374
N	0.35893	2832.1	1.179	0.261	2.52E-02	0.35893
Total outgoing LWR	0.36914	1148	0.46946	0.948	1.02E-02	0.36914

Table V. 8 Marginal tests of distLM model predicting the effect of environmental parameters on 16S rRNA gene and 16S cDNA stream on the Greenland Ice Sheet.

Variable	SS(trace)	Pseudo-F	P	Proportion explained
Day of year	6162.1	3.6281	0.001	0.10183
Total incoming SWR	7221.3	4.3363	0.001	0.11934
Total outgoing SWR	7268.8	4.3687	0.001	0.12012
Total incoming LWR	6693.9	3.9802	0.001	0.11062
Total outgoing LWR	6540.8	3.8782	0.001	0.10809
Total Melt	7401.9	4.4598	0.001	0.12232
SD incoming SWR	5894.8	3.4538	0.004	9.74E-02
SD outgoing SWR	6333	3.7405	0.004	0.10466
SD Melt	4845.2	2.7853	0.009	8.01E-02
Average outgoing SWR	5440.2	3.1611	0.01	8.99E-02
Average albedo	4882.2	2.8085	0.018	8.07E-02
Average incoming SWR	4181.2	2.3752	0.019	6.91E-02
SD outgoing LWR	3187.9	1.7796	0.09	5.27E-02
SD incoming LWR	3013.7	1.6773	0.104	4.98E-02
Average melt	2377.8	1.3089	0.185	3.93E-02
Average outgoing LWR	2274.5	1.2498	0.224	3.76E-02
Total weekly PDD	1770.2	0.96436	0.353	2.93E-02
Total weekly PDH	1731.5	0.94265	0.429	2.86E-02
Average incoming LWR	1592.7	0.86503	0.506	2.63E-02
SD albedo	1118.8	0.60278	0.82	1.85E-02
E	-3.94E-12	-2.09E-15	1	-6.52E-17
N	0	0	1	0

Table V. 9 Sequential tests of distLM model predicting the effect of environmental parameters on 16S rRNA gene and 16S cDNA stream on the Greenland Ice Sheet.

Variable	Adj R ²	SS(trace)	Pseudo-F	P	Proportion explained	Cumulative variance
Total Melt	0.12232	7401.9	4.4598	0.001	0.12232	0.12232
Total incoming LWR	0.20288	4874.4	3.1327	0.009	8.06E-02	0.20288
Total outgoing SWR	0.26461	3735.6	2.5184	0.032	6.17E-02	0.26461
Average incoming LWR	0.29103	1598.5	1.0805	0.33	2.64E-02	0.29103
Total weekly PDH	0.30971	1130.7	0.75797	0.579	1.87E-02	0.30971
SD outgoing LWR	0.32389	858.07	0.56628	0.797	1.42E-02	0.32389
Total incoming SWR	0.32389	-9.47E-12	0	1	-1.56E-16	0.32389
Day of year	0.32389	1.43E-11	0	1	2.36E-16	0.32389

Table V. 10 Marginal tests of distLM model predicting the effect of environmental parameters on all active taxa in cryoconite, snow and stream habitats on the Greenland Ice Sheet.

Variable	SS(trace)	Pseudo-F	P	Proportion explained
E	13497	5.5663	0.001	0.11008
N	10346	4.1468	0.005	8.44E-02
Day of year	8289.7	3.263	0.009	6.76E-02
SD outgoing SWR	8102.5	3.1841	0.019	6.61E-02
Total Melt	7639.7	2.9901	0.019	6.23E-02
Total incoming SWR	7517.8	2.9393	0.019	6.13E-02
Total incoming LWR	7046.1	2.7436	0.023	5.75E-02
Average outgoing SWR	7590.7	2.9697	0.025	6.19E-02
Average albedo	7011.4	2.7293	0.031	5.72E-02
Total outgoing SWR	7031.2	2.7375	0.035	5.73E-02
SD outgoing LWR	5685.8	2.1882	0.055	4.64E-02
Total outgoing LWR	5668.8	2.1814	0.06	4.62E-02
Average incoming SWR	5343.4	2.0504	0.06	4.36E-02
SD incoming LWR	3935.7	1.4923	0.18	3.21E-02
Average outgoing LWR	3617.4	1.368	0.213	2.95E-02
SD albedo	2721.4	1.0214	0.343	2.22E-02
SD Melt	2484.2	0.93056	0.431	2.03E-02
Average incoming LWR	2291.4	0.85699	0.464	1.87E-02
Total weekly PDD	2229.4	0.83338	0.509	1.82E-02
Average melt	2158.9	0.80655	0.517	1.76E-02
Total weekly PDH	2038	0.76059	0.533	1.66E-02
SD incoming SWR	2008.5	0.74941	0.534	1.64E-02

Table V. 11 Sequential tests of distLM model predicting the effect of environmental parameters on all active taxa in cryoconite, snow and stream habitats on the Greenland Ice Sheet.

Variable	Adj R ²	SS(trace)	Pseudo-F	P	Proportion explained	Cumulative variance
N	0.33226	13072	6.8651	0.001	0.10661	0.33226
Total Melt	0.22565	14171	6.567	0.001	0.11557	0.22565
E	0.11008	13497	5.5663	0.001	0.11008	0.11008
Total outgoing LWR	0.37449	5177.9	2.8355	0.016	4.22E-02	0.37449
Total incoming SWR	0.3957	2601.3	1.4394	0.152	2.12E-02	0.3957
SD Melt	0.41349	2180.8	1.213	0.265	1.78E-02	0.41349
SD outgoing SWR	0.4391	1575.3	0.87043	0.502	1.28E-02	0.4391
SD incoming LWR	0.42625	1564.6	0.8674	0.502	1.28E-02	0.42625

Table V. 12 Marginal tests of distLM model predicting the effect of environmental parameters on the rare active taxa in cryoconite, snow and stream habitats on the Greenland Ice Sheet.

Variable	SS(trace)	Pseudo-F	P	Proportion explained
E	13227	5.5051	0.002	0.1112
N	9971.8	4.0264	0.008	8.38E-02
SD outgoing SWR	7335.1	2.8918	0.016	6.17E-02
Day of year	7594.1	3.0009	0.022	6.38E-02
Total incoming SWR	6698.7	2.6259	0.027	5.63E-02
Average outgoing SWR	7054.8	2.7743	0.028	5.93E-02
Total Melt	6791.1	2.6643	0.029	5.71E-02
Total outgoing SWR	6214.3	2.4256	0.03	5.22E-02
Average albedo	6463.9	2.5286	0.041	5.43E-02
Total incoming LWR	6301.5	2.4615	0.049	5.30E-02
SD outgoing LWR	5608	2.1772	0.055	4.71E-02
Average incoming SWR	5181	2.0039	0.074	4.36E-02
Total outgoing LWR	4951.4	1.9112	0.087	4.16E-02
Average outgoing LWR	3680.8	1.4051	0.187	3.09E-02
SD incoming LWR	3325.8	1.2657	0.239	2.80E-02
SD albedo	2507.6	0.94762	0.41	2.11E-02
Total weekly PDD	2426.8	0.91646	0.423	2.04E-02
SD Melt	2474.6	0.93487	0.429	2.08E-02
Average incoming LWR	2296.9	0.86642	0.433	1.93E-02
Average melt	2256.3	0.8508	0.477	1.90E-02
Total weekly PDH	2236.2	0.84308	0.508	1.88E-02
SD incoming SWR	1845.5	0.69348	0.641	1.55E-02

Table V. 13 Sequential tests of distLM model predicting the effect of environmental parameters on the rare active taxa in cryoconite, snow and stream habitats on the Greenland Ice Sheet.

Variable	Adj R ²	SS(trace)	Pseudo-F	P	Proportion explained	Cumulative variance
N	0.32525	13241	6.9293	0.001	0.11132	0.32525
Total Melt	0.21393	12218	5.6193	0.001	0.10272	0.21393
E	0.1112	13227	5.5051	0.001	0.1112	0.1112
Total outgoing LWR	0.36805	5091	2.7769	0.015	4.28E-02	0.36805
Average melt	0.38925	2521.9	1.3887	0.184	2.12E-02	0.38925
SD Melt	0.40686	2094.2	1.1577	0.267	1.76E-02	0.40686
Total outgoing SWR	0.42281	1897.4	1.0503	0.351	1.60E-02	0.42281
SD incoming SWR	0.4308	950.05	0.51922	0.883	7.99E-03	0.4308
Total incoming SWR	0.4308	-1.12E-10	0	1	-9.44E-16	0.4308

APPENDIX VI

Publications arising from this thesis and associated work.

1. Gokul, J. K., Hodson, A. J., Saetnan, E. R., Irvine-Fynn, T. D. L., Westall, P. J., Detheridge, A. P., Takeuchi, N., Bussell, J. S., Mur, L. A. and Edwards, A. 2016. Taxon interactions control the distributions of cryoconite bacteria colonizing a High Arctic ice cap. *Molecular Ecology*, 25, 3752–3767.
2. Cook, J. M., Edwards, A., Bulling, M., Mur, L. A. J., Cook, S., Gokul, J. K., Cameron, K. A., Sweet, M. and Irvine-Fynn, T. D. L. 2016. Metabolome-mediated biocryomorphic evolution promotes carbon fixation in Greenlandic cryoconite holes. *Environmental Microbiology*, 18, 12, 4674-4686.
3. Rassner, S. M. E., Anesio, A. M., Girdwood, S. E., Hell, K., Gokul, J. K., Whitworth, D. E. and Edwards, A. 2016. Can the Bacterial Community of a High Arctic Glacier Surface Escape Viral Control? *Frontiers in Microbiology*, 7, 956.
4. Stibal, M., Gözdereliler, E., Cameron, K. A., Box, J. E., Stevens, I. T., Gokul, J. K., Schostag, M., Zarsky, J. D., Edwards, A., Irvine-Fynn, T. D. L. and Jacobsen, C. S. 2015. Microbial abundance in surface ice on the Greenland Ice Sheet. *Frontiers in Microbiology*, 6, 225.

Taxon interactions control the distributions of cryoconite bacteria colonizing a High Arctic ice cap

JARISHMA K. GOKUL,* ANDREW J. HODSON, † ‡ ELI R. SAETNAN,* TRISTRAM D. L. IRVINE-FYNN,§ PHILIPPA J. WESTALL,* ANDREW P. DETHERIDGE,* NOZOMU TAKEUCHI, JENNIFER BUSSELL,** LUIS A. J. MUR* and ARWYN EDWARDS *

*Institute of Biological, Rural and Environmental Sciences, Aberystwyth University, Cledwyn Building, Aberystwyth, SY23 3DD, UK, †Department of Geography, University of Sheffield, Sheffield, S10 2TN, UK, ‡Department of Arctic Geology, University Centre in Svalbard (UNIS), Longyearbyen, N-9171, Svalbard, UK, §Department of Geography and Earth Sciences, Aberystwyth University, Llandinam Building, Aberystwyth, SY23 3DB, UK, Department of Earth Sciences, Graduate School of Science, Chiba University, 1-33, Yayoicho, Inage-ku, Chiba, 263-8522, Japan, **University of Nottingham, Sutton Bonington Campus, Loughborough, Leicestershire LE12 5RD, UK

Abstract

Microbial colonization of glacial ice surfaces incurs feedbacks which affect the melting rate of the ice surface. Ecosystems formed as microbe–mineral aggregates termed cryoconite locally reduce ice surface albedo and represent foci of biodiversity and biogeochemical cycling. Consequently, greater understanding the ecological processes in the formation of functional cryoconite ecosystems upon glacier surfaces is sought. Here, we present the first bacterial biogeography of an ice cap, evaluating the respective roles of dispersal, environmental and biotic filtration occurring at local scales in the assembly of cryoconite microbiota. 16S rRNA gene amplicon semiconductor sequencing of cryoconite colonizing a Svalbard ice cap coupled with digital elevation modelling of physical parameters reveals the bacterial community is dominated by a ubiquitous core of generalist taxa, with evidence for a moderate pairwise distance–decay relationship. While geographic position and melt season duration are prominent among environmental predictors of community structure, the core population of taxa appears highly influential in structuring the bacterial community. Taxon co-occurrence network analysis reveals a highly modular community structured by positive interactions with bottleneck taxa, predominantly *Actinobacteria* affiliated to isolates from soil humus. In contrast, the filamentous cyanobacterial taxon (assigned to *Leptolyngbya/Phormidesmis priestleyi*) which dominates the community and binds together granular cryoconite are poorly connected to other taxa. While our study targeted one ice cap, the prominent role of generalist core taxa with close environmental relatives across the global cryosphere indicate discrete roles for cosmopolitan *Actinobacteria* and *Cyanobacteria* as respective keystone taxa and ecosystem engineers of cryoconite ecosystems colonizing ice caps.

Key words: bacteria, biogeography, cryoconite, ecosystem engineering, keystone species, Svalbard

Received 21 December 2015; revision received 16 May 2016; accepted 31 May 2016

Metabolome-mediated biocryomorphic evolution promotes carbon fixation in Greenlandic cryoconite holes

Joseph M. Cook,^{1,2} Arwyn Edwards,^{3*}
Mark Bulling,² Luis A. J. Mur,³ Sophie Cook,³
Jarishma K. Gokul,³ Karen A. Cameron,^{4,5} Michael
Sweet² and Tristram D. L. Irvine-Fynn⁶

¹Department of Geography, University of Sheffield,
Sheffield, S10 2TN, UK.

²Environmental Sustainability Research Centre, College
of Life and Natural Sciences, University of Derby, Derby,
DE22 1GB, UK.

³Institute of Biological, Environmental and Rural
Sciences, Aberystwyth University, Aberystwyth SY23
3DA, UK.

⁴Department of Geochemistry, Geological Survey of
Denmark and Greenland (GEUS), Copenhagen 1350,
Denmark.

⁵Center for Permafrost (CENPERM), University of
Copenhagen, Copenhagen 1350, Denmark.

⁶Centre for Glaciology, Department of Geography and
Earth Sciences, Aberystwyth University, Aberystwyth,
SY 23 3DB, UK.

metabolomics reveals concomitant shifts in cyclic AMP and fucose metabolism consistent with photo-taxis and extracellular polymer synthesis indicating metabolomic-level granular changes in response to perturbation. We present a conceptual model explaining this process and suggest that it results in remarkably robust net autotrophy on the Greenland Ice Sheet. We also describe observations of cryoconite migrating away from shade, implying a degree of self-regulation of carbon budgets over mesoscales. Since cryoconite is a microbe-mineral aggregate, it appears that microbial processes themselves form and maintain stable autotrophic habitats on the surface of the Greenland ice sheet.

Summary

Microbial photoautotrophs on glaciers engineer the formation of granular microbial-mineral aggregates termed cryoconite which accelerate ice melt, creating quasi-cylindrical pits called 'cryoconite holes'. These act as biogeochemical reactors on the ice surface and provide habitats for remarkably active and diverse microbiota. Evolution of cryoconite holes towards an equilibrium depth is well known, yet inter-actions between microbial activity and hole morphology are currently weakly addressed. Here, we experimentally perturbed the depths and diameters of cryoconite holes on the Greenland Ice Sheet. Cryoconite holes responded by sensitively adjusting their shapes in three dimensions ('biocryomorphic evolution') thus maintaining favourable conditions for net autotrophy at the hole floors. Non-targeted

Received 24 February, 2016; accepted 19 April, 2016. *For correspondence. E-mail aye@aber.ac.uk; Tel. 144(0)1970 622330



Can the Bacterial Community of a High Arctic Glacier Surface Escape Viral Control?

Sara M. E. Rassner^{1,2}, Alexandre M. Anesio³, Susan E. Girdwood¹, Katherina Hell⁴, Jarishma K. Gokul¹, David E. Whitworth¹ and Arwyn Edwards^{1*}

¹ Institute of Biological, Rural and Environmental Sciences, Aberystwyth University, Aberystwyth, UK, ² Department of Geography and Earth Sciences, Aberystwyth University, Aberystwyth, UK, ³ School of Geographical Sciences, Bristol Glaciology Centre, University of Bristol, Bristol, UK, ⁴ Institute of Ecology, University of Innsbruck, Innsbruck, Austria

Glacial ice surfaces represent a seasonally evolving three-dimensional photic zone which accumulates microbial biomass and potentiates positive feedbacks in ice melt. Since viruses are abundant in glacial systems and may exert controls on supraglacial bacterial production, we examined whether changes in resource availability would promote changes in the bacterial community and the dynamics between viruses and bacteria of meltwater from the photic zone of a Svalbard glacier. Our results indicated that, under ambient nutrient conditions, low estimated viral decay rates account for a strong viral control of bacterial productivity, incurring a potent viral shunt of a third of bacterial carbon in the supraglacial microbial loop. Moreover, it appears that virus particles are very stable in supraglacial meltwater, raising the prospect that viruses liberated in melt are viable downstream. However, manipulating resource availability as dissolved organic carbon, nitrogen, and phosphorous in experimental microcosms demonstrates that the photic zone bacterial communities can escape viral control. This is evidenced by a marked decline in virus-to-bacterium ratio (VBR) concomitant with increased bacterial productivity and number. Pyrosequencing shows a few bacterial taxa, principally *Janthinobacterium* sp., dominate both the source meltwater and microcosm communities. Combined, our results suggest that viruses maintain high VBR to promote contact with low-density hosts, by the manufacture of robust particles, but that this necessitates a trade-off which limits viral production. Consequently, dominant bacterial taxa appear to access resources to evade viral control. We propose that a delicate interplay of bacterial and viral strategies affects biogeochemical cycling upon glaciers and, ultimately, downstream ecosystems.

Keywords: glacier, meltwater, virus, viral shunt, bacterial diversity, vesicles

OPEN ACCESS

Edited by:

Brian D. Lanoil,
University of Alberta, Canada

Reviewed by:

Amy Michele Grunden,
North Carolina State University, USA
Jeremy Dodsworth,
California State University,
San Bernardino, USA

*Correspondence:

Arwyn Edwards
aye@aber.ac.uk

Specialty section:

This article was submitted to Extreme Microbiology, a section of the journal Frontiers in Microbiology

Received: 23 April 2016

Accepted: 02 June 2016

Published: 21 June 2016

Citation:

Rassner SME, Anesio AM, Girdwood SE, Hell K, Gokul JK, Whitworth DE and Edwards A (2016) Can the Bacterial Community of a High Arctic Glacier Surface Escape Viral Control? Front. Microbiol. 7:956. doi: 10.3389/fmicb.2016.00956

Microbial abundance in surface ice on the Greenland Ice Sheet

Marek Stibal^{1, 2, 3*}, Erkin Gözdereliler^{1, 2}, Karen A. Cameron^{1, 2}, Jason E. Box¹, Ian T. Stevens⁴, Jarishma K. Gokul⁴, Morten Schostag², Jakub D. Zarsky^{3, 5}, Arwyn Edwards⁴, Tristram D. L. Irvine-Fynn⁴ and Carsten S. Jacobsen^{1, 2, 6}

¹ Geological Survey of Denmark and Greenland, Copenhagen, Denmark, ² Center for Permafrost, University of Copenhagen, Copenhagen, Denmark, ³ Department of Ecology, Charles University in Prague, Prague, Czech Republic, ⁴ Centre for Glaciology, Aberystwyth University, Aberystwyth, UK, ⁵ Centre for Polar Ecology, University of South Bohemia, České Budějovice, Czech Republic, ⁶ Department of Plant and Environmental Sciences, University of Copenhagen, Copenhagen, Denmark

OPEN ACCESS

Edited by:

Catherine Larose,
University of Lyon, France

Reviewed by:

Marc Gregory Dumont, Max-Planck-Institute for Terrestrial Microbiology, Germany
Steffen Kolb,
University of Bayreuth, Germany

*Correspondence:

Marek Stibal, Department of Geochemistry, Geological Survey of Denmark and Greenland, Øster Voldgade 10, 1350 Copenhagen, Denmark
msti@geus.dk

Specialty section:

This article was submitted to Terrestrial Microbiology, a section of the journal Frontiers in Microbiology

Received: 11 January 2015

Paper pending published:
09 February 2015

Accepted: 06 March 2015

Published: 24 March 2015

Citation:

Stibal M, Gözdereliler E, Cameron KA, Box JE, Stevens IT, Gokul JK, Schostag M, Zarsky JD, Edwards A, Irvine-Fynn TDL and Jacobsen CS (2015) Microbial abundance in surface ice on the Greenland Ice Sheet. *Front. Microbiol.* 6:225. doi: 10.3389/fmicb.2015.00225

Measuring microbial abundance in glacier ice and identifying its controls is essential for a better understanding and quantification of biogeochemical processes in glacial ecosystems. However, cell enumeration of glacier ice samples is challenging due to typically low cell numbers and the presence of interfering mineral particles. We quantified for the first time the abundance of microbial cells in surface ice from geographically distinct sites on the Greenland Ice Sheet (GrIS), using three enumeration methods: epifluorescence microscopy (EFM), flow cytometry (FCM), and quantitative polymerase chain reaction (qPCR). In addition, we reviewed published data on microbial abundance in glacier ice and tested the three methods on artificial ice samples of realistic cell (10^2 – 10^7 cells ml⁻¹) and mineral particle (0.1–100 mg ml⁻¹) concentrations, simulating a range of glacial ice types, from clean subsurface ice to surface ice to sediment-laden basal ice. We then used multivariate statistical analysis to identify factors responsible for the variation in microbial abundance on the ice sheet. EFM gave the most accurate and reproducible results of the tested methodologies, and was therefore selected as the most suitable technique for cell enumeration of ice containing dust. Cell numbers in surface ice samples, determined by EFM, ranged from $\sim 2 \times 10^3$ to $\sim 2 \times 10^6$ cells ml⁻¹ while dust concentrations ranged from 0.01 to 2 mg ml⁻¹. The lowest abundances were found in ice sampled from the accumulation area of the ice sheet and in samples affected by fresh snow; these samples may be considered as a reference point of the cell abundance of precipitants that are deposited on the ice sheet surface. Dust content was the most significant variable to explain the variation in the abundance data, which suggests a direct association between deposited dust particles and cells and/or by their provision of limited nutrients to microbial communities on the GrIS.

Keywords: glacier ice, microbial abundance, Greenland Ice Sheet, epifluorescence microscopy, flow cytometry, quantitative PCR, multivariate analysis

